SOURCE DATA   TRANSPARENT PROCESS

THE EMBO JOURNAL

USP33 deubiquitinates and stabilizes HIF-2alpha to promote hypoxia response in glioma stem cells

Aili Zhang[1], Zhi Huang[1], Weiwei Tao[1], Kui Zhai[1], Qiulian Wu[2], Jeremy N Rich[2], Wenchao Zhou[1,*] & Shideng Bao[1,3,4,**]

Abstract

Hypoxia regulates tumor angiogenesis, metabolism, and therapeutic response in malignant cancers including glioblastoma, the most lethal primary brain tumor. The regulation of HIF transcriptional factors by the ubiquitin–proteasome system is critical in the hypoxia response, but hypoxia-inducible deubiquitinases that counteract the ubiquitination remain poorly defined. While the activation of ERK1/2 also plays an important role in hypoxia response, the relationship between ERK1/2 activation and HIF regulation remains elusive. Here, we identified USP33 as essential deubiquitinase that stabilizes HIF-2alpha protein in an ERK1/2-dependent manner to promote hypoxia response in cancer cells. USP33 is preferentially induced in glioma stem cells by hypoxia and interacts with HIF-2alpha, leading to its stabilization through deubiquitination. The activation of ERK1/2 upon hypoxia promoted HIF-2alpha phosphorylation, enhancing its interaction with USP33. Silencing of USP33 disrupted glioma stem cells maintenance, reduced tumor vascularization, and inhibited glioblastoma growth. Our findings highlight USP33 as an essential regulator of hypoxia response in cancer stem cells, indicating a novel potential therapeutic target for brain tumor treatment.

Introduction

Hypoxia promotes malignant progression of solid tumors by activating neovascularization, altering metabolism, enhancing therapeutic resistance, increasing pro-tumor inflammation, and

supporting the maintenance of cancer stem cells (Li *et al*, 2009, 2014; Rankin & Giaccia, 2016; Semenza, 2016; Stegen *et al*, 2019). Cellular response to hypoxia is dominantly regulated by the hypoxia-inducible factors (HIFs; Palazon *et al*, 2012, 2017; Fan *et al*, 2014; Shukla *et al*, 2017). The ubiquitin–proteasome system plays a central role in hypoxia response and HIF protein stabilization (LaGory & Giaccia, 2016). Deubiquitinases (DUBs) are the main enzymes responsible for protein deubiquitination and stabilization, but the functional regulation of DUBs in response to hypoxia remains elusive. In the hypoxic niches in glioblastoma (GBM), glioma stem cells (GSCs) are enriched to promote therapeutic resistance and malignant progression (Li *et al*, 2009; Seidel *et al*, 2010; Man *et al*, 2018). Whereas HIF1α is universally induced in glioma cells under hypoxic conditions, HIF2α is preferentially elevated in GSCs (Li *et al*, 2009; Seidel *et al*, 2010; Man *et al*, 2018), suggesting that GSCs may have developed unique adaptive mechanisms including the induction of DUBs in response to hypoxia.

There are around 100 DUBs in human cells, and the largest subgroup, the ubiquitin-specific protease (USP), consists of approximately 60 members (Clague *et al*, 2019; Mennerich *et al*, 2019). The relatively small number of DUBs counterbalance approximately 600 E3 ubiquitin ligases in regulating the ubiquitin–proteasome system, highlighting the importance of DUBs in both normal and cancer cells (Clague *et al*, 2019; Mennerich *et al*, 2019). Several studies have suggested that DUBs play crucial roles in the maintenance of normal and cancer stem cells. In neural progenitor cells (NPCs), USP7 stabilizes the repressor element 1 silencing transcription factor (REST) through deubiquitination and is required for maintaining neural progenitor cells (NPCs; Huang *et al*, 2011). Likewise, USP13 reverses the polyubiquitination of c-Myc in GSCs to promote GSC self-renewal and GBM growth (Fang *et al*, 2017). However, little is known about the DUBs involved in the hypoxia response in caner stem cells such as GSCs.

In response to hypoxic stress, the HIF family of transcriptional factors predominantly direct cellular adaption to hypoxia. HIFs function as heterodimers containing an oxygen-sensitive α unit and a constitutively expressed β unit (Semenza, 2012). HIF1α is

---

1 Department of Cancer Biology, Lerner Research Institute, Cleveland Clinic, Cleveland, OH, USA
2 Hillman Cancer Center, University of Pittsburgh Medical Center, Pittsburgh, PA, USA
3 Case Comprehensive Cancer Center, Case Western Reserve University School of Medicine, Cleveland, OH, USA
4 Center for Cancer Stem Cell Research, Lerner Research Institute, Cleveland Clinic, Cleveland, OH, USA
 *Corresponding author. Tel: +1 2166360631; E-mail: wenchao.m.zhou@gmail.com
 **Corresponding author (lead contact). Tel: +1 2166351009; E-mail: baos@ccf.org

ubiquitously expressed in all extant metazoan species, whereas HIF2α expression is restricted to certain tissues and cell types (Tian *et al*, 1997; Li *et al*, 2009; Loenarz *et al*, 2011). Although HIF1α and HIF2α bind to similar hypoxia-responsive elements (HREs), they occupy distinct genomic sites and are not functionally interchangeable (Forsythe *et al*, 1996; Hu *et al*, 2003; Branco-Price *et al*, 2012). Normoxia promotes hydroxylation of the HIFα unit to facilitate the binding of the von Hippel-Lindau (VHL) E3 ubiquitin ligase, resulting in proteasomal degradation of HIFα proteins (Kaelin & Ratcliffe, 2008). Hypoxia abrogates the hydroxylation of HIFα proteins and the consequent VHL binding to increase the stability of HIFs (Kaelin & Ratcliffe, 2008). As the reverse process of ubiquitination, deubiquitination of HIFα has not been defined. A handful of DUBs, such as USP20, have been discovered to catalyze deubiquitination of HIF1α (Li *et al*, 2005; Troilo *et al*, 2014; Wu *et al*, 2016; Sun *et al*, 2018). However, most of these DUBs seem to promote deubiquitination of HIF1α in a hypoxia-independent manner (Altun *et al*, 2012; Flugel *et al*, 2012; Bremm *et al*, 2014; Troilo *et al*, 2014; Wu *et al*, 2016). Moreover, our previous study suggested that HIF1α is only stabilized under acute hypoxic conditions, but HIF2α is induced even under modest hypoxia (Li *et al*, 2009), indicating that HIF2α and HIF1α may be regulated through different mechanisms.

Beside the upregulation of HIF proteins, the activation of ERK1/2 kinases in response to hypoxia has been noticed for a while (Minet *et al*, 2000; Li *et al*, 2008; Lee *et al*, 2015). In fact, the concomitant elevation of HIF and ERK1/2 activities converge to promote malignant phenotypes in cancers (Franovic *et al*, 2009; Zhuo *et al*, 2019). The activation of ERK1/2 is closely associated with the upregulation of HIFs under hypoxic conditions. ERK1/2 activation seems to be an earlier event in hypoxia response and often a prerequisite for HIF1α accumulation (Li *et al*, 2008; Choi *et al*, 2010). In line with a possible direct effect of ERK1/2 on HIF proteins, HIF1α is phosphorylated under hypoxia in an ERK1/2-dependent manner (Minet *et al*, 2000). However, the potential role of ERK1/2 in regulating HIF2α in cancer stem cells in response to hypoxia remains elusive.

Due to the critical impact of hypoxia on malignant tumors and the central role of the ubiquitination–deubiquitination system in regulating hypoxia response, the DUBs participating in hypoxia response in cancer stem cells could be promising druggable targets. In this study, we aim to identify the key hypoxia-inducible DUB for HIF2α stabilization in GSCs. We found that USP33 was markedly upregulated in GSCs in response to hypoxia, and validated the preferential expression of USP33 in GSCs in the hypoxic niches in GBM tumors. We further demonstrated that USP33 interacted with HIF2α to deubiquitinate and stabilize HIF2α upon hypoxia. Interestingly, the activation of ERK1/2 upon hypoxia executes phosphorylation of S484 on HIF2α to promote the interaction between USP33 and HIF2α, resulting in deubiquitination of HIF2α. Importantly, silencing USP33 in GSCs abolished hypoxia response, disrupted GSC maintenance, and inhibited GBM tumor growth, leading to a markedly increased survival of tumor-bearing animals. The discovery of USP33 as an upstream DUB directly regulating HIF2α in an ERK1/2-dependent manner not only offers new insights into the initiation of hypoxia response but may also have translational impact on cancer treatment.

Results

USP33 is a hypoxia-inducible deubiquitinase preferentially expressed in GSCs

To identify potential hypoxia-inducible deubiquitinases in GSCs, we cultured GSCs under hypoxic and normoxic conditions and examined the change in protein levels of a cohort of deubiquitinases. Our previous studies showed that HIF2α is upregulated specifically in GSCs, whereas HIF1α is elevated in both GSCs and the matched non-stem tumor cells (NSTCs) in response to hypoxia, suggesting that the induction of HIF2α rather than HIF1α may reflect the unique hypoxic responses in GSCs (Li *et al*, 2009). We initially determined HIF2α protein levels in GSCs cultured at different oxygen concentrations and found that the maximal upregulation of HIF2α was achieved under 5% oxygen, whereas the HIF1α induction occurred under oxygen concentrations lower than 3% (Fig EV1A). Therefore, we examined the potential induction of deubiquitinases in GSCs at 5% oxygen. Immunoblot and qPCR analyses showed that only USP33 but no other tested deubiquitinases was induced by the hypoxic condition (5% oxygen) in GSCs (Figs 1A and EV1B, Appendix Fig S1A–D). Interestingly, USP33 protein levels achieved maximal upregulation within 12 h under 5% oxygen in most tested GSC lines, whereas HIF2α protein levels were slightly induced in 12 h but markedly upregulated in 24 h under the same hypoxic condition (Fig 1A), suggesting that hypoxia induction of USP33 was prior to that of HIF2α in GSCs. Similar to HIF2α, USP33 was induced by a wide range of hypoxic conditions (1–5% oxygen) (Figs 1A and B, and EV1A). To examine the hypoxia-induced upregulation of USP33 in GSCs in human GBMs, we performed immunofluorescent staining of USP33, the hypoxia marker CA9, and the GSC marker SOX2 on primary human GBM sections (Fig 1C). While only a fraction of CA9- or SOX2-positive cells showed USP33 staining, the majority of CA9/SOX2 double-positive cells had strong USP33 staining (Fig 1C and D), indicating that USP33 was upregulated in those GSCs under hypoxia in human GBMs. To further confirm the upregulation of USP33 in the hypoxic niches in GBM, we treated mice bearing intracranial GSC-derived GBM tumors with pimonidazole HCl to label the hypoxic cells and then examined USP33 protein levels. Two hours after tail vein injection of pimonidazole HCl, mice were sacrificed and GBM tumors were subjected to analysis. As expected, immunofluorescent staining showed that pimonidazole-positive areas were enriched with HIF1α and HIF2α signals (Fig EV1C–F), demonstrating the correct labeling of hypoxic niches by pimonidazole *in vivo*. Consistently, USP33 staining was highly enriched in pimonidazole-positive areas (Fig 1E and F), indicating that USP33 upregulation mainly occurred in hypoxic niches in GBM tumors. Moreover, treatment with CoCl$_2$ that mimics hypoxic conditions also upregulated USP33 protein levels in multiple GSC lines (Fig EV1G). These data indicate that hypoxia upregulates USP33 protein levels in GSCs in GBMs.

Previous reports showed that GSCs had higher HIF2α expression than matched NSTCs even under regular culture conditions and that HIF2α was required for the GSC maintenance (Li *et al*, 2009). Consistently, immunoblot analyses of paired GSCs and NSTCs cultured under normoxic conditions demonstrated relatively higher protein levels of both USP33 and HIF2α in GSCs (Fig EV1H), suggesting that higher expression of this hypoxia-inducible DUB
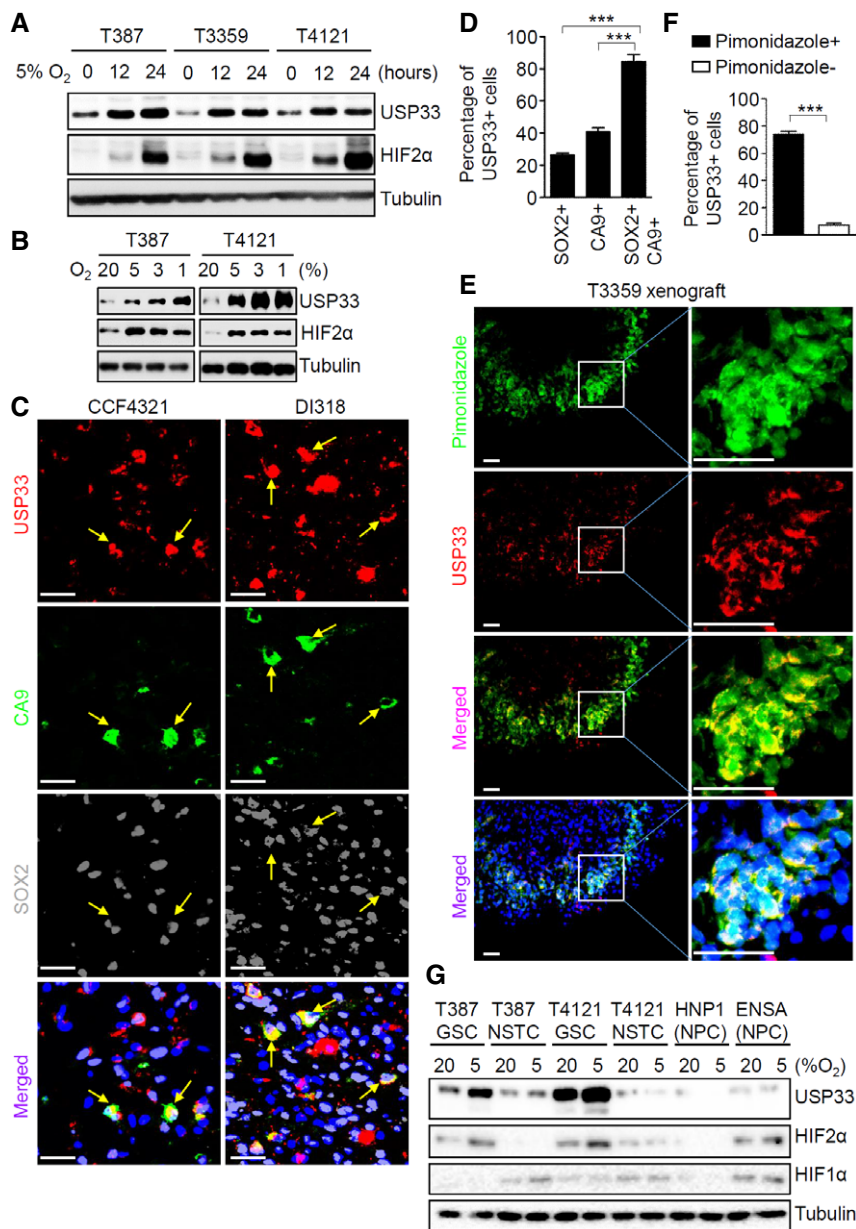
Figure 1. USP33 is a hypoxia-inducible deubiquitinase that is preferentially expressed in GSCs.

A Immunoblot analysis of USP33 and HIF2α protein levels in GSCs cultured under 5% oxygen for different times. GSCs (T387, T3359, and T4121) were cultured under 5% oxygen for 0, 12, or 24 h before harvest. Dramatic induction of USP33 was observed at 12 h under 5% oxygen. HIF2α protein levels were slightly upregulated at 12 h and further elevated at 24 h under 5% oxygen.

B Immunoblot analysis of USP33 and HIF2α protein levels in GSCs cultured in different concentrations of oxygen. GSCs were cultured under 20%, 5%, 3%, or 1% oxygen for 24 h before harvest. Induction of USP33 was observed under 5%, 3%, and 1% oxygen.

C Immunofluorescent analyses of USP33 (red), the hypoxia marker CA9 (green), and the stem cell marker SOX2 (gray) in human primary GBMs. Arrows indicate the USP33$^+$/CA9$^+$/SOX2$^+$ cells. Scale bar, 80 μm.

D Statistical quantification of (C) showing the ratio of USP33$^+$ cells in SOX2$^+$, CA9$^+$, or SOX2$^+$/CA9$^+$ cells in human primary GBMs. USP33 expression was detected in a fraction of GSCs (SOX2$^+$) or CA9$^+$ hypoxic cells, but the majority of the hypoxic GSCs (SOX2$^+$/CA9$^+$ cells) were USP33$^+$, indicating that USP33 was induced in GSCs in response to hypoxia. (n = 5 sections; ***$P < 0.001$; mean ± s.e.m.; two-tailed unpaired t-test).

E Immunofluorescent analyses of USP33 (red) and the hypoxic cell population labeled by pimonidazole (green) in intracranial xenografts derived from T3359 GSCs. Mice bearing intracranial xenografts were injected intravenously (tail vein) with 60 mg/kg of pimonidazole and were sacrificed 2 h post-injection. Hypoxic cells were labeled with the FITC-conjugated mouse monoclonal anti-pimonidazole antibody. Scale bar, 80 μm.

F Statistical quantification of (E) showing the percentage of USP33$^+$ cells in the pimonidazole$^+$ hypoxic and the pimonidazole$^-$ normoxic cells. The majority of hypoxic cell population in GSC-derived xenografts were positively stained for USP33. (n = 5 tumors; ***$P < 0.001$; mean ± s.e.m.; two tailed unpaired t-test).

G Immunoblot analysis of USP33, HIF2α, and HIF1α protein levels in GSCs, NSTCs, and NPCs in normoxic and hypoxic conditions. Hypoxia (5% O$_2$) relative to normoxia (20% O$_2$) clearly induced USP33 and HIF2α expression in GSCs but not NSTCs or NPCs. The mild hypoxia of 5% O$_2$ showed negligible induction of HIF1α in all cells.

Source data are available online for this figure.

may also be required for GSC maintenance. As HIF2α is preferentially induced in GSCs but not in NSTCs, hypoxia-responsive signaling may be cell type specific (Li *et al*, 2009). Similarly, hypoxia-induced upregulation of USP33 was clearly detected in GSCs but not in NSTCs or NPCs (Figs 1G and EV1G,I,J). Taken together, USP33 is preferentially expressed by GSCs under normoxic condition and further upregulated under hypoxia in GSCs *in vitro* and *in vivo*.

USP33 stabilizes HIF2α proteins in GSCs in response to hypoxia

Because USP33 is induced under hypoxia preferentially in GSCs, we speculated that USP33 functioning as a deubiquitinase may stabilize its downstream targets specifically in GSCs. USP33 shares an approximately 59% identity with the HIF1α deubiquitinase USP20,

indicating the possible regulation of HIFs by USP33 (Li *et al*, 2005). Our previous studies showed that HIF1α was induced in both GSCs and NSTCs, but HIF2α expression was elevated preferentially in GSCs in response to hypoxia (Li *et al*, 2009). The preferential induction of USP33 in GSCs rather than NSTCs or NPCs is consistent with the HIF2α induction pattern in response to hypoxia (Figs 1G and EV1G,I and J). In addition, 5% oxygen mildly upregulated HIF2α mRNA levels but dramatically increased HIF2α protein levels (Fig 1A, Appendix Fig S2A), suggesting a potential post-translational stabilization of HIF2α in GSCs in response to hypoxia at 5% oxygen. Moreover, the USP33 protein levels increased ahead of HIF2α induction in response to hypoxia at 5% oxygen (Fig 1A) but declined behind HIF2α degradation when returning to normoxia (Appendix Fig S2B), suggesting a longer turnover of USP33 relative
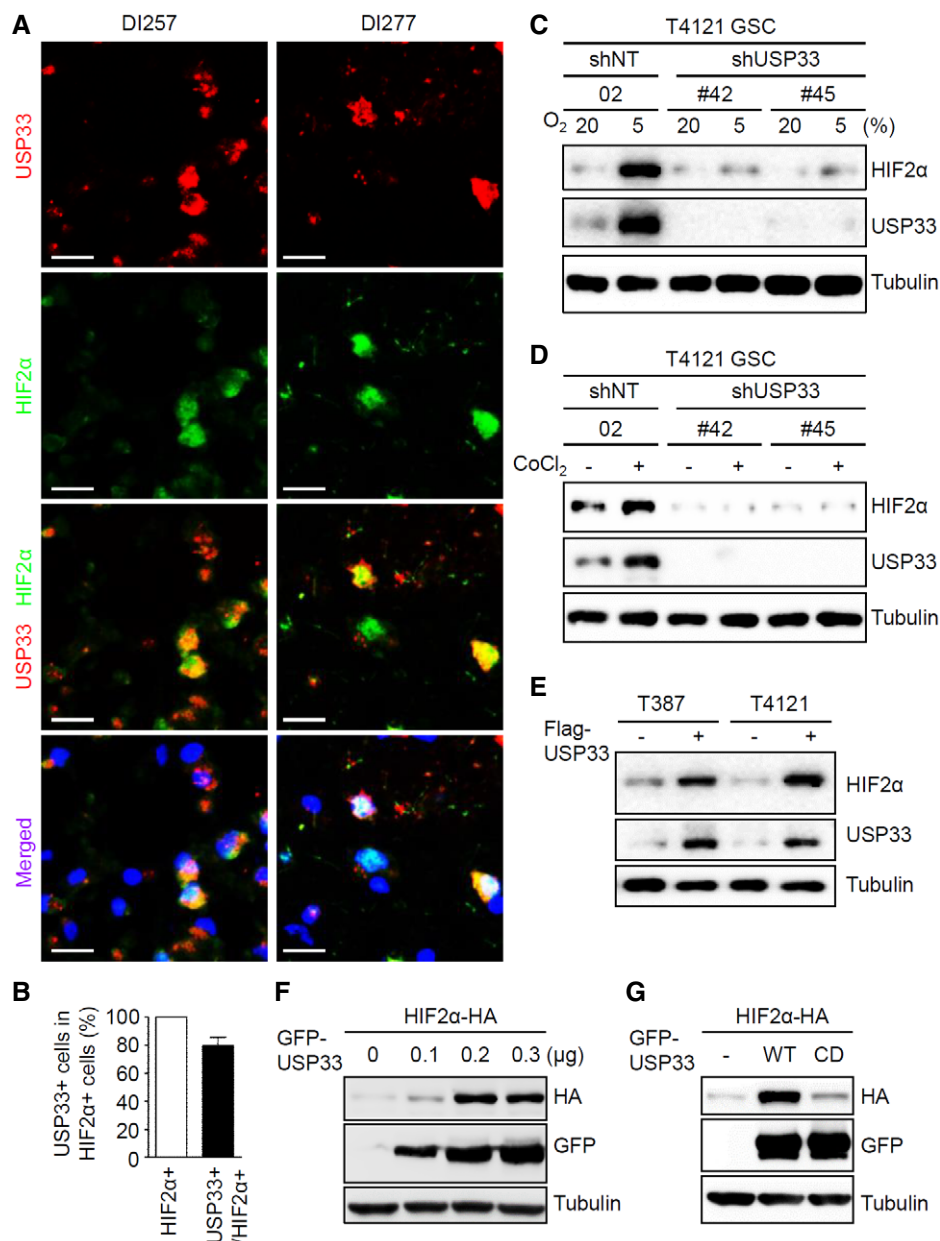

Figure 2.

Figure 2. USP33 stabilizes HIF2α protein in GSCs.

A, B   Representative images (A) and statistical quantification (B) of immunofluorescent analyses of USP33 (red) and HIF2α (green) in human primary GBMs. Frozen sections of human GBMs were immunostained with antibodies against USP33 and HIF2α, and counterstained with DAPI to show nuclei (blue). The percentage of USP33$^+$ cells in the HIF2α$^+$ population was quantified. The majority of HIF2α$^+$ cells were positively stained for USP33 in human GBMs. Scale bar, 40 μm. (n = 5 sections; mean ± s.e.m).

C   Immunoblot analysis of HIF2α induction in T4121 GSCs expressing shUSP33 or shNT in response to low oxygen. Twenty-four hours post-lentiviral transduction of shUSP33 or shNT, GSCs were incubated under 20% or 5% oxygen for 24 h and then harvested for the immunoblot analysis. Disruption of USP33 abrogated HIF2α induction in GSCs in response to 5% oxygen.

D   Immunoblot analysis of HIF2α induction in T4121 GSCs expressing shNT or shUSP33 in response to CoCl₂-mimicking hypoxia. Twenty-four hours post-lentiviral transduction of shUSP33 or shNT, GSCs were treated with CoCl₂ (300 μM) for 12 h and then harvested for the immunoblot analysis. Disruption of USP33 abrogated CoCl₂-induced HIF2α expression in GSCs.

E   Immunoblot analysis of HIF2α protein levels in GSCs expressing ectopic Flag-tagged USP33 in normoxia. Cells were transduced with lentiviruses carrying Flag-tagged USP33 or the control vector, followed by two rounds of puromycin selection. Ectopic expression of USP33 elevated HIF2α protein levels in GSCs cultured under 20% oxygen.

F   Immunoblot analysis of ectopic HIF2α protein levels in 293T cells with gradually increased amount of ectopic USP33. 0.5 μg of HA-tagged HIF2α plasmids together with the increased amounts of GFP-tagged USP33 plasmids (0, 0.1, 0.2, or 0.3 μg) were introduced into 293T cells. Forty-eight hours post-transfection, levels of ectopic HIF2α-HA and GFP-USP33 were analyzed by immunoblot analysis. Concomitantly increased levels of ectopic HIF2α and USP33 expression indicated the positive regulation of HIF2α protein by USP33.

G   Immunoblot analysis of ectopic HIF2α protein levels in 293T cells expressing ectopic wild-type (WT) USP33 or the catalytically dead (CD) USP33. HA-tagged HIF2α plasmids (0.5 μg) were introduced into 293T cells alone or together with GFP-tagged WT or CD USP33 plasmids (0.2 μg). Levels of ectopic HIF2α-HA and GFP-USP33 were analyzed 48 h post-transfection. Expression of the wild-type USP33 but not the catalytically dead USP33 increased the ectopic HIF2α protein levels.

Source data are available online for this figure.

to HIF2α proteins during the hypoxia response. Thus, we sought to explore the possible association between USP33 and HIF2α. We initially determined the correlation between HIF2α and USP33 expression in human primary GBMs. Immunofluorescent analyses showed that the majority of HIF2α-positive cells had USP33 staining (Fig 2A and B), suggesting a positive correlation between HIF2α and USP33. We then disrupted the endogenous USP33 in GSCs and examined the induction of HIF2α under hypoxic conditions. Immunoblot analyses showed that disruption of USP33 almost abolished HIF2α induction in response to either 5% oxygen or CoCl₂ treatment (Fig 2C and D, Appendix Fig S2C–F), indicating that USP33 is required for HIF2α induction under hypoxic conditions in GSCs. Consistently, ectopic overexpression of USP33 in GSCs elevated endogenous HIF2α protein levels under normoxic conditions (Fig 2E), suggesting that USP33 is able to upregulate HIF2α levels in GSCs. We further explored the USP33-mediated stabilization of HIF2α proteins by ectopic expression of USP33 and HIF2α under the control of CMV promoter in 293T cells, which excluded the involvement of transcriptional regulation. Immunoblot analyses showed that USP33 expression increased HIF2α protein levels in a dose-dependent manner (Fig 2F), indicating that USP33 upregulates HIF2α at the protein level but not at the mRNA level. To further clarify whether USP33 affects HIF2α protein synthesis or degradation, 293T cells expressing ectopic HIF2α with or without USP33 were treated with the translation inhibitor cycloheximide. Immunoblot analyses demonstrated that overexpression of USP33 delayed the decline in HIF2α protein levels, while HIF2α protein levels declined rapidly after cycloheximide treatment in the control cells without USP33 expression (Appendix Fig S2G), suggesting that USP33 controls HIF2α protein stability. We next determined whether the deubiquitinase activity of USP33 is required for HIF2α stabilization. Whereas ectopic expression of the wild-type USP33 upregulated the protein levels of HIF2α, ectopic expression of the catalytically dead USP33 (C194S/H673Q) mutant (Berthouze *et al*, 2009; Niu *et al*, 2020) largely lost the capacity to elevate HIF2α levels (Fig 2G), indicating that the USP33 deubiquitinase activity is

essential for the USP33-mediated stabilization of HIF2α protein in GSCs. Of note, ectopic overexpression of USP33 in NSTCs upregulated the levels of HIF2α protein to a much less extent than that in GSCs (Fig 2E, Appendix Fig S2H), indicating that USP33 may have a stronger potency to stabilize HIF2α proteins in GSCs. Finally, treatment with the proteasome inhibitor MG132 markedly restored the HIF2α protein levels in GSCs transduced with shUSP33 shRNAs under hypoxia (Appendix FigsS2I and J). Taken together, our data demonstrate that USP33 stabilizes HIF2α protein in GSCs in response to hypoxia.

USP33 interacts with HIF2α and deubiquitinates HIF2α in GSCs in response to hypoxia

As USP33 is a deubiquitinase that stabilizes HIF2α protein in GSCs, we sought to determine whether HIF2α is a substrate of USP33. We initially investigated the interaction between HIF2α and USP33 in GSCs. Immunoprecipitation analyses showed that whereas HIF2α had a weak interaction with USP33 under normoxic conditions, hypoxia treatment with 5% oxygen or CoCl₂ dramatically increased the interaction between HIF2α and USP33 (Figs 3A–D and EV2A–C), indicating that HIF2α is complexed with USP33 under hypoxic conditions. Furthermore, ubiquitination assays showed a strong polyubiquitination of the endogenous HIF2α in GSCs under the normoxic condition (20% oxygen), but ectopic overexpression of USP33 remarkably reduced the polyubiquitination of HIF2α (Fig 3E). Moreover, whereas the endogenous HIF2α showed weak polyubiquitination in GSCs under 5% oxygen, disruption of USP33 markedly elevated the polyubiquitination of HIF2α (Figs 3F and EV2D), indicating that USP33 mediates the deubiquitination of HIF2α under hypoxic conditions in GSCs. Collectively, these data demonstrate that USP33 interacts with and deubiquitinates HIF2α to stabilize HIF2α protein in GSCs in response to hypoxia.

To further confirm the functional interaction between USP33 and HIF2α, we next examined whether key mutations on human USP33 and HIF2α proteins affect their interaction. We applied the

catalytically dead USP33 (C194S/H673Q) mutant (USP33-CD) (Berthouze *et al*, 2009; Niu *et al*, 2020), as well as the HIF2α-2dPA (P405A/P531A) mutant that lost the binding capacity to the ubiquitin E3 ligase VHL (Yan *et al*, 2007). Interestingly, the catalytically dead USP33-CD mutant showed a much stronger interaction with HIF2α relative to the wild-type USP33 (Figs 3G and EV2E). In addition, compared with the wild-type HIF2α, the HIF2α-2dPA mutant showed a much weaker interaction with USP33 (Figs 3H and EV2F). Whereas the ectopic HIF2α was heavily polyubiquitinated in 293T cells, co-expression of the wild-type USP33 but not the USP33-CD mutant dramatically reduced polyubiquitination of HIF2α

(Fig EV2G). Likewise, due to the lack of VHL binding, the HIF2α-2dPA mutant had a much weaker polyubiquitination relative to the wild-type HIF2α (Fig EV2H). Thus, we speculated that the polyubiquitin chains on HIF2α proteins might enhance the interaction between HIF2α and USP33. To test this possibility, we examined the ubiquitination of the HIF2α proteins co-immunoprecipitated with USP33 in GSCs and found a strong ubiquitin signal at the molecular weight of HIF2α (Fig EV2I), indicating that those HIF2α proteins complexed with USP33 are ubiquitinated. In summary, these data suggest that USP33 binds to the ubiquitinated HIF2α protein to deubiquitinate HIF2α.
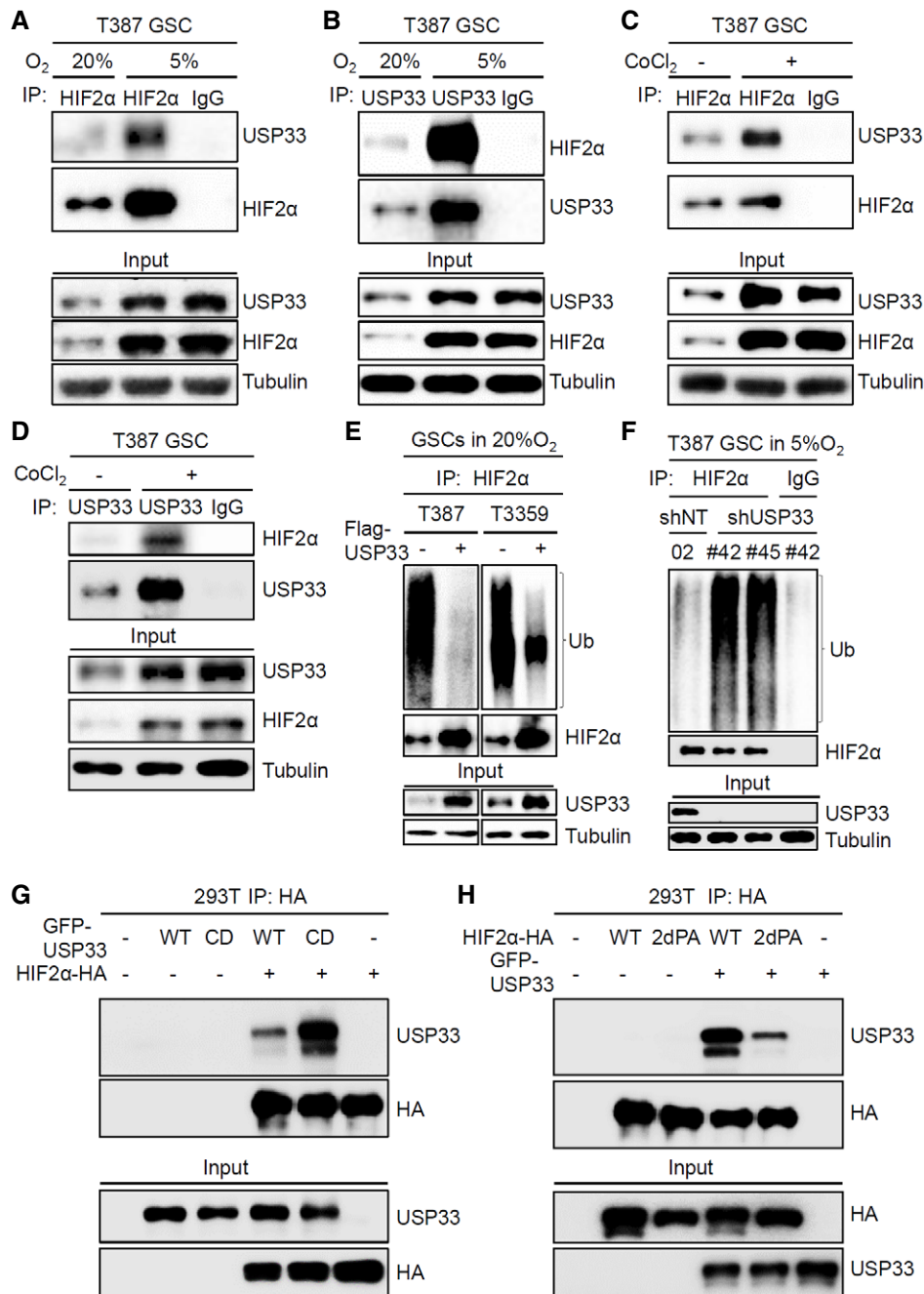

Figure 3.

Figure 3. USP33 interacts with and deubiquitinates HIF2α in GSCs.

A, B   Co-immunoprecipitation (Co-IP) to detect the interaction between endogenous HIF2α and USP33 in GSCs in response to low oxygen. GSCs were cultured under 20% or 5% oxygen for 24 h before harvest for the Co-IP. Cell lysate was subjected to immunoprecipitation with anti-HIF2α (A) or anti-USP33 (B) antibodies. Co-immunoprecipitated products were immunoblotted with the indicated antibodies. An increased interaction between HIF2α and USP33 was detected in GSCs cultured under 5% oxygen relative to 20% oxygen.

C, D   Co-immunoprecipitation (Co-IP) to detect the interaction between endogenous HIF2α and USP33 in GSCs in response to CoCl₂ treatment. GSCs were treated with CoCl₂ (300 μM) for 12 h before harvest for the Co-IP. Cell lysate was subjected to immunoprecipitation with anti-HIF2α (C) or anti-USP33 (D) antibodies. Co-immunoprecipitated products were immunoblotted with the indicated antibodies. An increased interaction between HIF2α and USP33 was detected in GSCs treated with CoCl₂-mimicking hypoxia.

E   Immunoblot analysis of the polyubiquitination of endogenous HIF2α proteins in GSCs with or without ectopic USP33 expression. Flag-tagged USP33 was introduced into GSCs through lentiviral infection. Forty-eight hours post-infection, GSCs were treated with MG132 (20μM) for 6 h and then harvested for ubiquitination assays. Cell lysate was subjected to immunoprecipitation with anti-HIF2α antibodies followed by immunoblot with anti-Ub antibodies. Ectopic expression of USP33 resulted in a remarkable decrease in polyubiquitination of HIF2α in GSCs cultured under 20% oxygen.

F   Immunoblot analysis of the polyubiquitination of endogenous HIF2α proteins in GSCs expressing shUSP33 or shNT in response to low oxygen. Twenty-four hours post-lentiviral infection, GSCs were incubated in 5% oxygen for 24 h before harvest. MG132 (20μM) was added to cell culture 6 h before harvest for the ubiquitination assay. Cell lysate was subjected to immunoprecipitation with anti-HIF2α antibodies followed by immunoblot with anti-Ub antibodies. Disruption of USP33 elevated polyubiquitination of HIF2α in GSCs cultured under 5% oxygen.

G   Co-immunoprecipitation to detect the interaction between HIF2α and the wild-type (WT) or the catalytically dead (CD) USP33. Ectopic HA-tagged HIF2α were expressed in 293T cells with GFP-tagged wild-type or catalytically dead USP33. Cell lysates were subjected to immunoprecipitation with anti-HA antibodies. Co-immunoprecipitated products immunoblotted with the indicated antibodies. The catalytically dead USP33 relative to the wild-type USP33 showed a stronger affinity to HIF2α.

H   Co-immunoprecipitation to determine the interaction between USP33 and the wild-type (WT) HIF2α or the P405A-P531A (2dPA) HIF2α mutant that lacks hydroxylation. Ectopic GFP-tagged USP33 and HA-tagged WT or 2dPA HIF2α were expressed in 293T cells. Cell lysates were subjected to immunoprecipitation with anti-HA antibodies. Co-immunoprecipitated products were immunoblotted with the indicated antibodies. The 2dPA HIF2α mutant relative to the wild-type HIF2α showed a weaker affinity to USP33.

Source data are available online for this figure.

The activation of ERK1/2 upon hypoxia promotes phosphorylation of S484 on HIF2α to facilitate its interaction with USP33

As USP33 interacts with HIF2α and deubiquitinates HIF2α in GSCs under hypoxic conditions, we next investigated the hypoxia-responsive molecular events mediating the interaction between HIF2α and USP33. Protein interaction is frequently facilitated by post-translational modifications such as phosphorylation. Since previous reports have described the serine/threonine phosphorylation (pS/T) of HIF2α (Conrad *et al*, 1999; Pangou *et al*, 2016; Gkotinakou *et al*, 2019), we examined the pS/T status of endogenous HIF2α in GSCs under normoxic and hypoxic conditions. Immunoblot analyses showed that 5% oxygen treatment remarkably elevated the pS/T of HIF2α (Fig 4A). As previous studies showed that hypoxia induced activation of the serine/threonine kinases ERK1/2 (Stalmans *et al*, 2015; Masson *et al*, 2019) that executed the phosphorylation of HIF2α (Gkotinakou *et al*, 2019), we analyzed the activation of ERK1/2 and found that ERK1/2 were strongly phosphorylated in GSCs under 5% oxygen (Fig 4A). We then sought to determine whether activated ERK1/2 are involved in the pS/T of HIF2α to impact the interaction between HIF2α and USP33. Surprisingly, we found that inhibition of ERK1/2 activity with the MEK kinase inhibitor U0126 dramatically reduced the pS/T of endogenous HIF2α in GSCs under hypoxic conditions (Figs 4B and EV3A). Moreover, immunoprecipitation analyses demonstrated a striking decrease in the interaction between HIF2α and USP33 in GSCs after U0126 treatment (Figs 4C and D and EV3A). Similarly, a specific ERK1/2 inhibitor LY3214996 disrupted the interaction between HIF2α and USP33 in GSCs under hypoxia (Fig EV3B). These data indicated that the ERK1/2-dependent pS/T of HIF2α facilitates the interaction between HIF2α and USP33 in GSCs in response to hypoxia. In line with the reduced HIF2α binding to

USP33 after U0126 treatment, suppression of ERK1/2 activity greatly restored polyubiquitination of HIF2α in GSCs treated with 5% oxygen or CoCl₂ (Figs 4E and EV3C and D). These results demonstrate that the ERK1/2-mediated pS/T of HIF2α is required for the interaction of HIF2α with USP33 and the deubiquitination of HIF2α in GSCs in response to hypoxia.

We next sought to determine the potential pS/T sites on human HIF2α protein that are critical for facilitating the interaction between HIF2α and USP33. As the ectopic HIF2α protein in 293T cells also exhibited the ERK1/2-dependent pS/T (Fig EV3E), and suppression of the pS/T of the ectopic HIF2α by U0126 treatment interrupted its interaction with the ectopic USP33 (Fig EV3F and G), the pS/T of ectopic HIF2α in 293T cells could functionally mimic the pS/T of endogenous HIF2α in GSCs. We therefore used the ectopic expression system to explore the pS/T sites on HIF2α protein as the target of ERK1/2. It has been shown that ERK1/2 substrates often contain a minimal consensus motif Ser/Thr-Pro with a preference for proline at −2 positions (Gonzalez *et al*, 1991). In line with this motif, we identified serine 484 and serine 581 on human HIF2α protein as two potential phosphorylation sites, and thus generated the S484A- and S581A-HIF2α mutants by converting serine to alanine. Immunoprecipitation analyses showed that the S484A-HIF2α mutant showed the weakest binding to USP33 relative to the wild-type HIF2α and the S581A HIF2α mutant (Fig 4F and G), while the S484A/S581A double mutations on HIF2α could not further attenuate HIF2α binding to USP33 (Fig 4F and G). These results indicated that S484 on human HIF2α is the key phosphorylation site responsible for mediating the interaction between HIF2α and USP33. Taken together, our data demonstrate that hypoxia activates ERK1/2 kinases, which in turn phosphorylate the S484 site on HIF2α to facilitate its interaction with USP33, resulting in deubiquitination and stabilization of HIF2α protein in GSCs in response to hypoxia.

USP33 is required for the maintenance of GSCs

Because USP33 is a hypoxia-inducible DUB preferentially expressed in GSCs and further induced under hypoxia, we further interrogated the role of USP33 in the GSC maintenance under normoxic and hypoxic conditions. Tumorsphere formation assays showed that USP33 disruption (shUSP33) inhibited GSC tumorsphere formation even under normoxic conditions (Fig 5A and B, Appendix Fig S3A and B). Moreover, hypoxia markedly enhanced the inhibitory effect of USP33 disruption on GSC tumorsphere formation, leading to a

further decrease in both size and number of tumorspheres cultured under 5% oxygen relative to those under 20% oxygen (Fig 5A–D, Appendix Fig S3A–D). In addition, cell titer assays showed that USP33 disruption reduced cell proliferation of GSCs under both normoxic and hypoxic conditions (Fig 5E, Appendix Fig S3E). Consistently, immunofluorescent staining of the apoptotic marker cleaved caspase-3 demonstrated that disruption of USP33 in GSCs induced cell apoptosis under normoxic conditions and more severe apoptosis under hypoxic conditions (Fig 5F and G, Appendix Fig S3F and G). Annexin V staining further confirmed the elevated
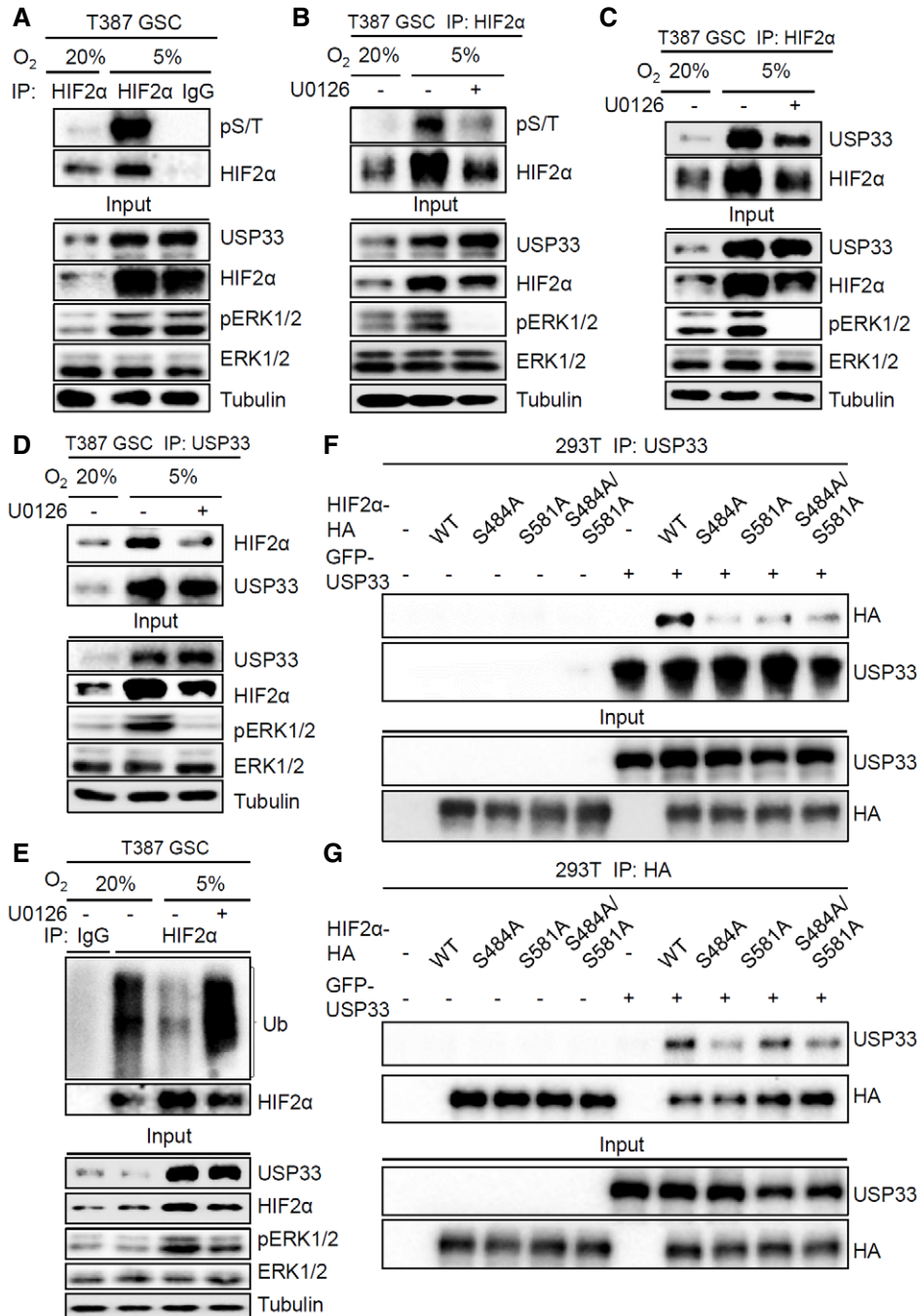

Figure 4.

◀

Figure 4. The activation of ERK1/2 upon hypoxia promotes the serine phosphorylation on HIF2α to facilitate its interaction with USP33.

A   Immunoblot analysis of the serine/threonine phosphorylation (pS/T) status of HIF2α in GSCs in response to 5% oxygen. GSCs were cultured under 20% or 5% oxygen for 24 h, and then harvested for immunoprecipitation with anti-HIF2α antibodies or IgG control. Immunoprecipitated endogenous HIF2α were immunoblotted with anti-pan-pS/T antibodies. An increased pS/T of HIF2α was detected in GSCs cultured under 5% oxygen relative to 20% oxygen.

B   Immunoblot analysis of the serine/threonine phosphorylation (pS/T) status of HIF2α in GSCs after inhibition of ERK1/2 activity. GSCs were cultured under 20% or 5% oxygen for 24 h, then treated with the MEK inhibitor U0126 (10 μM) for 30 min to inhibit ERK1/2 activity, and harvested for immunoprecipitation with anti-HIF2α antibodies. Immunoprecipitated endogenous HIF2α were immunoblotted with anti-pan-pS/T antibodies. In comparison with 20% oxygen treatment, the treatment with 5% oxygen elevated pS/T of HIF2α in GSCs, but the increased pS/T of HIF2α was abolished by U0126 treatment.

C, D   Co-immunoprecipitation to detect the interaction between endogenous HIF2α and USP33 in GSCs after inhibition of ERK1/2 activity. GSCs were cultured under 20% or 5% oxygen for 24 h, then treated with the MEK inhibitor U0126 (10 μM) for 30 min to inhibit ERK1/2 activity, and harvested for immunoprecipitation with anti-HIF2α (C) or anti-USP33 (D) antibodies. Co-immunoprecipitated products were immunoblotted with the indicated antibodies. Relative to 20% oxygen treatment, 5% oxygen treatment promoted the interaction between HIF2α and USP33 in GSCs. However, inhibition of ERK1/2 activity by U0126 treatment suppressed the interaction between HIF2α and USP33.

E   Immunoblot analysis of the polyubiquitination of endogenous HIF2α proteins in GSCs after inhibition of ERK1/2 activity. GSCs were cultured under 20% or 5% oxygen for 24 h before harvest. MG132 (20 μM) was added to cell culture 6 h before harvest, and U0126 (10 μM) was added to cell culture 30 min before harvest. Cell lysates were subjected to immunoprecipitation with anti-HIF2α antibodies and immunoblot with anti-Ub antibodies. Whereas 5% oxygen suppressed the polyubiquitination of HIF2α, inhibition of ERK1/2 activity by U0126 restored the polyubiquitination of HIF2α in GSCs.

F, G   Co-immunoprecipitation to determine the serine phosphorylation sites in human HIF2α responsible for its binding to USP33. Ectopic GFP-tagged USP33 along with HA-tagged wild-type HIF2α or HIF2α mutants with indicated serine-to-alanine point mutations were expressed in 293T cells. Cell lysates were subjected to immunoprecipitation with anti-USP33 antibodies (F) or anti-HA agaroses (G). Co-immunoprecipitated products were immunoblotted with the indicated antibodies. The S484A mutation largely attenuated the interaction of HIF2α with USP33, indicating that the serine 484 site in HIF2α was the most important phosphorylation site for the interaction between HIF2α and USP33.

Source data are available online for this figure.

apoptosis of GSCs after disruption of USP33 under normoxic and hypoxic conditions (Appendix Fig S4). Furthermore, limiting dilution assays demonstrated that disruption of USP33 reduced the clonogenic abilities of GSCs (Fig EV4A and B). In contrast, disruption of USP33 showed negligible effects on the proliferation of NSTCs (Appendix Fig S5A). Moreover, when GSCs were forced to overexpress ectopic HIF2α, the inhibitory effects of USP33 disruption on GSC proliferation and tumorsphere formation were markedly attenuated under normoxic and hypoxic conditions (Fig EV4C–F, Appendix Fig S5B), indicating that the functions of USP33 were mediated by HIF2α. Consistently, disruption of USP33 inhibited the transcription of the HIF2α target genes EPO and VEGFA in GSCs under hypoxia (Appendix Fig S5C), suggesting the suppression of HIF2α downstream signaling in the absence of USP33. Collectively, these data indicate that USP33 is required for the GSC maintenance under both normoxic and hypoxic conditions, particularly under hypoxic conditions.

Disrupting USP33 impairs hypoxia response and inhibits GBM tumor growth

Inadequate oxygen supply during the rapid tumor growth triggers the formation of hypoxic niches in the tumor microenvironment. In order to adapt to the hypoxic stress, tumor cells in the hypoxic niches have to sense the hypoxic condition and initiate hypoxia responses. As USP33 expression is induced by hypoxia, we next investigated the role of USP33 in initiating hypoxia response in GBM tumors. In order to monitor the activation of hypoxia response within hypoxic niches, we constructed a reporter system containing a destabilized GFP (d2GFP) fluorescent reporter under the control of four repetitive cis-acting hypoxia-responsive elements (HREs) followed by a minimum CMV promoter (4HRE-d2GFP) (Vordermark *et al*, 2001) (Fig 6A). GSCs transduced with the 4HRE-d2GFP reporter displayed strong green fluorescent signals under 5% oxygen but not under 20% oxygen (Fig 6B), representing a successfully monitoring of the activated hypoxia response in GSCs. Thus, in

GBM tumors derived from the GSCs transduced with 4HRE-d2GFP, tumor cells within the hypoxic niches with activated hypoxia response would express green fluorescent signals. Whereas a considerable fraction of tumor cells in the control GBM tumors displayed GFP expression, representing activation of hypoxia response, disruption of USP33 in GSCs resulted in a dramatic reduction in tumor cells with GFP signals (Fig 6C and D), indicating that USP33 disruption impairs hypoxia response in GBM tumors derived from shUSP33-expressing GSCs. Interestingly, immunofluorescent analyses showed much more GFP signals in SOX2-positive relative to SOX2-negative populations in the tumor mass, suggesting that stronger hypoxia response occurred in GSCs relative to NSTCs (Fig 6E and F, Appendix Fig S6A–D). Moreover, immunofluorescent staining of the apoptotic marker cleaved caspase-3 showed much less apoptosis in the GFP-positive tumor area (hypoxia) relative to GFP-negative tumor area (normoxia) (Fig 6G and H). TUNEL assays confirmed that cell apoptosis intended to occur in the hypoxic areas (Appendix Fig S6E and F). These results suggested that activated hypoxia response in tumor cells may protect glioma cells from apoptosis. Collectively, these data indicate that USP33 mediates the hypoxia response in tumor cells within the hypoxic niches in GBM tumors.

Because USP33 is involved in hypoxia response in the hypoxic niches that play a critical role in GBM malignant progression (Li *et al*, 2009; Seidel *et al*, 2010; Man *et al*, 2018), we next investigated the function of USP33 in GSC-derived GBM tumor growth by silencing USP33. GSCs expressing luciferase and shUSP33 or shNT (non-targeting shRNA) control were implanted into mouse brains, and intracranial tumor growth was monitored with bioluminescent imaging. *In vivo* bioluminescent imaging showed that disruption of USP33 in GSCs inhibited tumor growth of GSC-derived GBM xenografts (Figs 7A and EV5A). Consistently, the mice bearing xenografts derived from shUSP33-expressing GSCs had significantly longer survival than the control group (Figs 7B and EV5B). Immunofluorescent staining of cleaved caspase-3 and Ki67 demonstrated that disruption of USP33 dramatically elevated apoptosis (Figs 7C and D, and EV5C and D) but inhibited cell proliferation

(Figs 7E and F, and EV5E and F) in GBM tumors. TUNEL assays further proved the elevated cell apoptosis in the xenografts derived from shUSP33-expressing GSCs relative to the control xenografts (Appendix Fig S7A–C). Meanwhile, immunofluorescent analyses demonstrated the reduced HIF2α and USP33 expression in the xenografts derived from shUSP33-expressing GSCs relative to the control xenografts (Appendix Fig S7D–H). As hypoxia promotes tumor angiogenesis (Mukhopadhyay et al, 1995; West et al, 2010), we also determined the vascularization in the GSC-derived xenografts. Immunofluorescent analyses with the endothelial cell marker Glut1

showed that disruption of USP33 significantly inhibited tumor vascularization in GBM tumors derived from shUSP33-expressing GSCs (Fig 7G and H). Taken together, these data demonstrate that disrupting USP33 inhibits GBM growth.

Discussion

Hypoxia is closely associated with therapeutic resistance across multiple solid tumors (Fluegen et al, 2017; Shukla et al, 2017; Ma
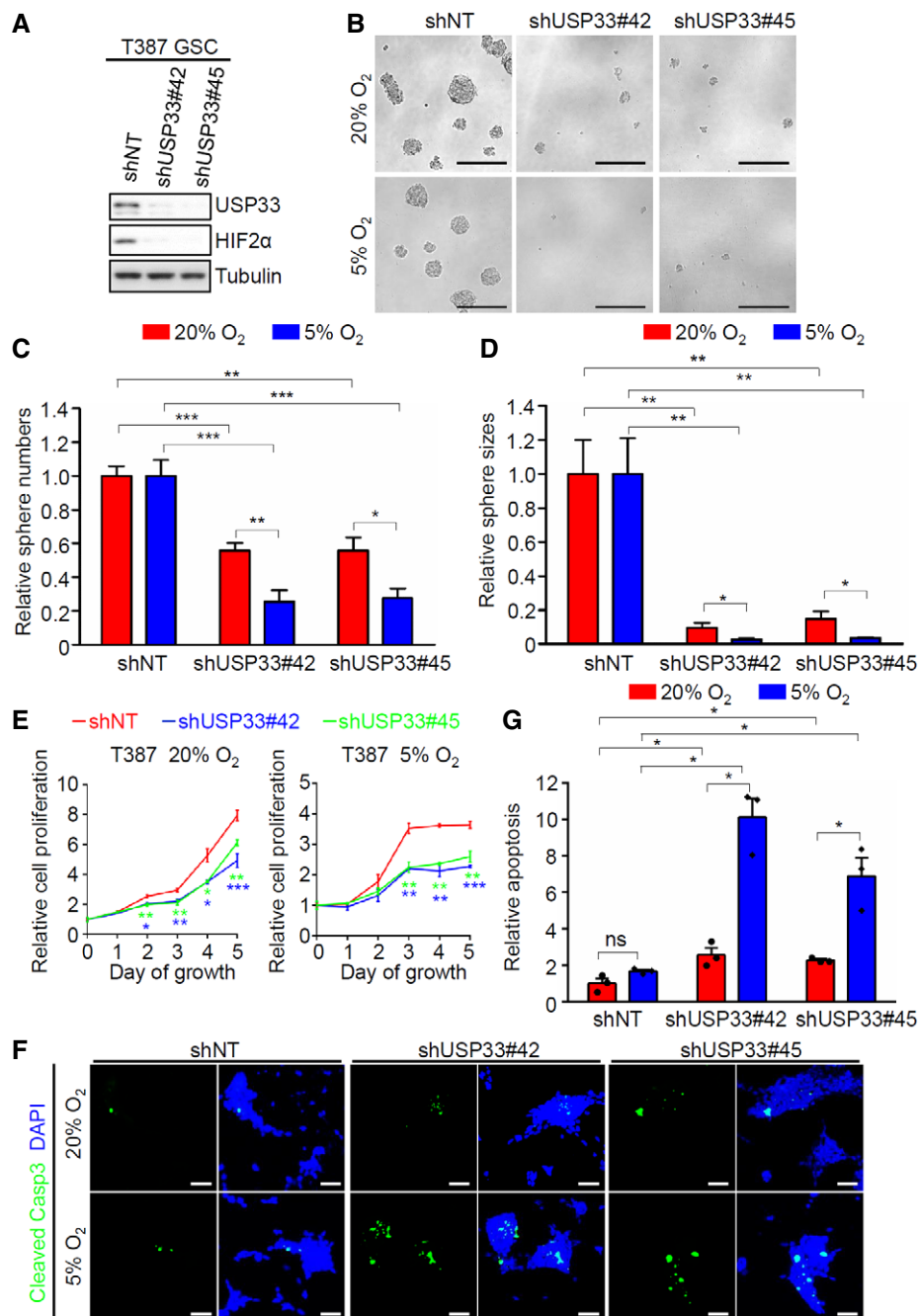

Figure 5.

Figure 5. USP33 is required for maintaining GSC self-renewal potential under hypoxic and normoxic conditions.

A   Immunoblot analysis of USP33 and HIF2α protein levels in T387 GSCs expressing USP33-targeting shRNAs (shUSP33) or non-targeting shRNA (shNT). Targeting USP33 by two distinct shRNA clones through lentiviral infection reduced USP33 and HIF2α expression in GSCs.

B   Representative images of tumorsphere formation of T387 GSCs expressing USP33-targeting shRNA (shUSP33) or non-targeting shRNA (shNT). Twenty-four hours after lentiviral infection, T387 GSCs expressing shUSP33 or shNT were planted in 96-well plates at the density of 2,000 cells per well and cultured for 48 h under normoxia (20% O_2) or hypoxia (5% O_2). Disruption of USP33 inhibited GSC tumorsphere formation in normoxia and dramatically suppressed GSC tumorsphere formation in hypoxia. Scale bar, 200 μm.

C, D   Statistical quantifications of tumorsphere numbers (C) and sizes (D) showing the inhibition of tumorsphere formation after disruption of USP33 in T387 GSCs. Disruption of USP33 inhibited tumorsphere formation of GSCs in normoxia, whereas hypoxia further augmented the inhibitory effects of USP33 disruption on GSC tumorsphere formation. Data represent three independent experiments. The presented bars for tumorsphere numbers and sizes were based on 5 and 10 technical replicates, respectively. *$P < 0.05$; **$P < 0.01$; ***$P < 0.001$ (mean ± s.e.m.; two tailed unpaired t-test).

E   Cell titer assays showing cell growth of T387 GSCs expressing shUSP33 or shNT in normoxia or hypoxia. GSCs were transduced with shNT or shUSP33 through lentiviral infection for 24 h, and then split into 96-well plates at the concentration of 2,000 cells per well. Cell titer was determined by the Glo luminescent cell viability assay kit (Promega) at the indicated time points. Disruption of USP33 inhibited GSC growth in normoxia and hypoxia. The experiment has been repeated three times. The presented curves were based on three technical replicates. *$P < 0.05$; **$P < 0.01$; ***$P < 0.001$ (mean ± s.e.m.; two-tailed unpaired t-test).

F   Representative immunofluorescent staining of the apoptotic marker cleaved caspase-3 in T387 GSCs expressing shUSP33 or shNT in normoxia or hypoxia. GSCs were attached to hESC-Qualified Matrix (Corning) in six-well plates at the concentration of 50,000 cells per well. Forty-eight hours post-infection with shUSP33 or shNT lentiviruses, cells were stained for cleaved caspase-3 (green) and nuclei (blue). Scale bar, 80 μm.

G   Statistical quantification of (F) showing relative apoptosis of T387 GSCs expressing shUSP33 or shNT in normoxia or hypoxia. Disruption of USP33 increased the apoptosis of GSCs in normoxia, which was further elevated in hypoxia. Data represent three independent experiments. *$P < 0.05$ (mean ± s.e.m.; two-tailed unpaired t-test).

Source data are available online for this figure.

et al, 2019). Various types of cells including tumor cells, endothelial cells, and immune cells have been found to respond to hypoxia, resulting in profound changes in pro-tumor vascularization, metabolism, and immunosuppression (Palazon *et al*, 2012, 2017; Fan *et al*, 2014; Shukla *et al*, 2017). However, the diverse phenotypes are commonly under the control of the HIFs (Palazon *et al*, 2012, 2017; Fan *et al*, 2014; Shukla *et al*, 2017). Although the downstream effectors of HIFs vary in different types of cells, HIF proteins are widely recognized as the initiating point of hypoxia response (Palazon *et al*, 2012; Palazon *et al*, 2017; Stegen *et al*, 2019; van den Beucken *et al*, 2014). On the other hand, few upstream regulators of HIFs have been reported, and they often function in a hypoxia-independent fashion (Fan *et al*, 2014; Lee *et al*, 2016). The investigation of a hypoxia-induced upstream regulator of HIFs not only provides new therapeutic targets but also expands our understanding of the initiation of hypoxia response at the molecular level.

Protein ubiquitination and deubiquitination play central roles in hypoxia response. In general, hypoxia reduces the O_2-dependent hydroxylation, abrogates the binding of the E3 ligase VHL, and thus prevents the polyubiquitination and proteasomal degradation of hypoxia-responsive proteins (Kaelin & Ratcliffe, 2008). In this scenario, the loss of the polyubiquitination signals on hypoxia-responsive proteins is mainly a passive and gradual process. Alternatively, DUB-mediated deubiquitination represents an active and timely process for the removal of the polyubiquitin chains to stabilize hypoxia-responsive proteins, which may function to finely tune the strength and duration of hypoxia signaling (Clague *et al*, 2019). Importantly, hypoxia is also associated with the maintenance of both normal stem cells and cancer stem cells. DUBs have been shown to regulate cell pluripotency and differentiation. In neural stem cells, the pivotal transcriptional factor REST is under the control of USP7, USP14, and USP15 (Huang *et al*, 2011; Doeppner *et al*, 2013; Faronato *et al*, 2013). Moreover, USP22 and USP13 regulate the stability of the stem cell transcriptional factor c-Myc (Fang *et al*, 2017; Kim *et al*, 2017). As tumor cells incline to transit into a stem cell-like status under hypoxic stress (Fluegen *et al*, 2017; van

den Beucken *et al*, 2014), the induction of DUBs may bestow the pluripotency of cancer cells in the hypoxic niches. Whereas tumor cells generally respond to hypoxia, DUBs may be selectively regulated by hypoxia in specific cancer cell subpopulations such as cancer stem cells in the hypoxic niche.

Elevated expression of HIFs was found to be associated with poor clinical outcomes in cancer patients with cervical, breast, ovarian, renal, lung, and brain cancers (Birner *et al*, 2000; Giatromanolaki *et al*, 2001; Holmquist-Mengelbier *et al*, 2006; Klatte *et al*, 2007; Osada *et al*, 2007; Helczynska *et al*, 2008). Upregulation of HIFs may have resulted from the loss or inhibition of the VHL activity, the inhibition of the upstream hydrolyses, the increase in mRNA levels, and the enhanced translation of HIF mRNAs (Li *et al*, 2009; Bett *et al*, 2013; Zhang *et al*, 2016; Kokate *et al*, 2018). However, HIFα proteins have an expeditious turnover with a half-life about 5 min (Doe *et al*, 2012; Zhuang *et al*, 2016), highlighting the importance of the DUB-mediated deubiquitination as an active mechanism in regulating HIFα protein levels. HIF1α and HIF2α have non-interchangeable functions and they are expressed in different tumor cell subpopulations with disparate regulations (Keith *et al*, 2011). In GBM, HIF1α is expressed in most glioma cells but HIF2α is preferentially expressed in GSCs (Li *et al*, 2009). In addition, whereas HIF1α is accumulated under acute hypoxic conditions, HIF2α is the dominant hypoxia-inducible factor present in GSCs in response to a wide range of low oxygen levels (Li *et al*, 2009). A short list of DUBs such as USP20, USP28, and USP9X have been reported to regulate HIF1α in response to hypoxia because they counteract polyubiquitination of HIF1α mediated by VHL (Li *et al*, 2005; Troilo *et al*, 2014; Goto *et al*, 2015; Zhang *et al*, 2016; Sun *et al*, 2018). However, no convincing DUBs to execute the deubiquitination of HIF2α proteins have been reported. Although USP8 is reported to interact with and stabilize HIF2α proteins, the deubiquitination of HIF2α by USP8 has not been demonstrated (Troilo *et al*, 2014). OTUD7B is found to upregulate the transcription of HIF2α, which is irrelevant to the deubiquitination of HIF2α proteins (Bremm *et al*, 2014; Moniz *et al*, 2015). Our study identified USP33 as a key DUB of HIF2α under
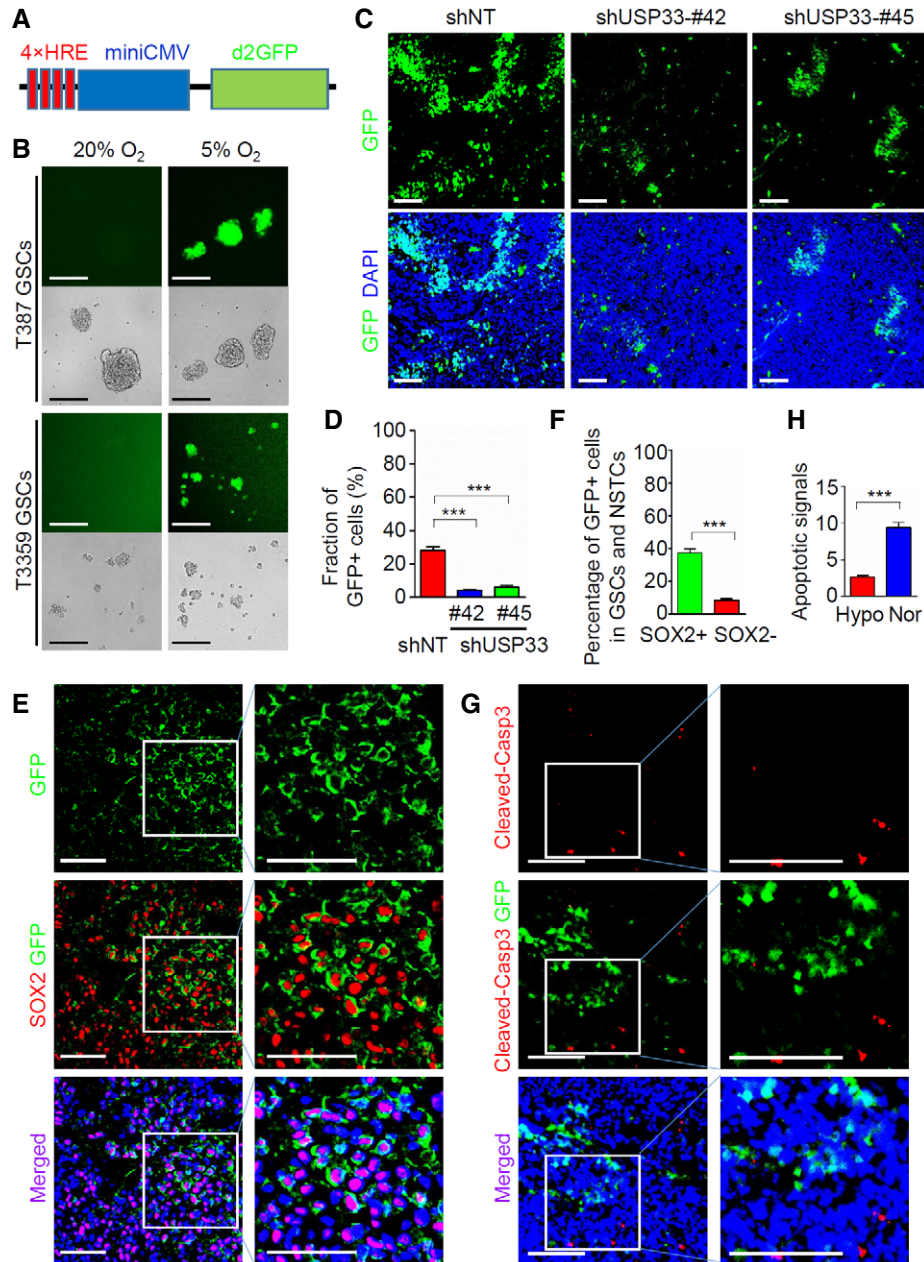
Figure 6. Disrupting USP33 impairs hypoxia response in GSCs in the tumor microenvironment.

A   A schematic diagram of the 4HRE-d2GFP fluorescent hypoxia reporter system containing a destabilized GFP (d2GFP) fluorescent reporter under the control of four repetitive cis-acting hypoxia-responsive elements (HRE) followed by a minimum CMV promoter. The hypoxia reporter system was constructed on the backbone of pCDH-CMV-MCS-EF1α-Neo lentiviral vector (System Biosciences).

B   Representative images of autonomous fluorescent signals from T387 and T3359 GSCs transduced with 4HRE-d2GFP in response to 5% oxygen. Strong GFP signals were detected under 5% oxygen, whereas no GFP signal was detected under 20% oxygen. Scale bar, 200 μm.

C, D   Representative images (C) and statistical quantifications (D) of autonomous fluorescent signals of 4HRE-d2GFP in xenografts derived from or shUSP33- or shNT-expressing T387 GSCs transduced with 4HRE-d2GFP. The reduced fraction of GFP$^+$ tumor cells in the xenografts derived from shUPS33-expressing GSCs relative to the control xenografts indicated that USP33 disruption impaired hypoxia response in tumor cells. Scale bar, 200 μm. ***$P < 0.001$ ($n = 5$ tumors; mean $\pm$ s.e.m.; two-tailed unpaired t-test).

E, F   Representative images (E) and statistical quantifications (F) of autonomous fluorescent signals of 4HRE-d2GFP (green) and immunofluorescent staining of the stem cell marker SOX2 (red) in xenografts derived from T387 GSCs transduced with 4HRE-d2GFP. More GFP signals were detected in the SOX2$^+$ cells compared with the SOX2$^-$ cells, suggesting a stronger hypoxia response in GSCs relative to NSTCs. Scale bar, 200 μm. ***$P < 0.001$ ($n = 5$ tumors; mean $\pm$ s.e.m.; two-tailed unpaired t-test).

G, H   Representative images (G) and statistical quantifications (H) of immunofluorescent staining of the apoptotic marker cleaved caspase-3 (red) and autonomous fluorescent signals of 4HRE-d2GFP (green) in xenografts derived from T387 GSCs transduced with 4HRE-d2GFP. The GFP$^+$ population had much less apoptosis relative to the GFP$^-$ population, suggesting that hypoxia response inhibited cell apoptosis. Scale bar, 200 μm. ($n = 5$ tumors for each group; ***$P < 0.001$; mean $\pm$ s.e.m.; two-tailed unpaired t-test).
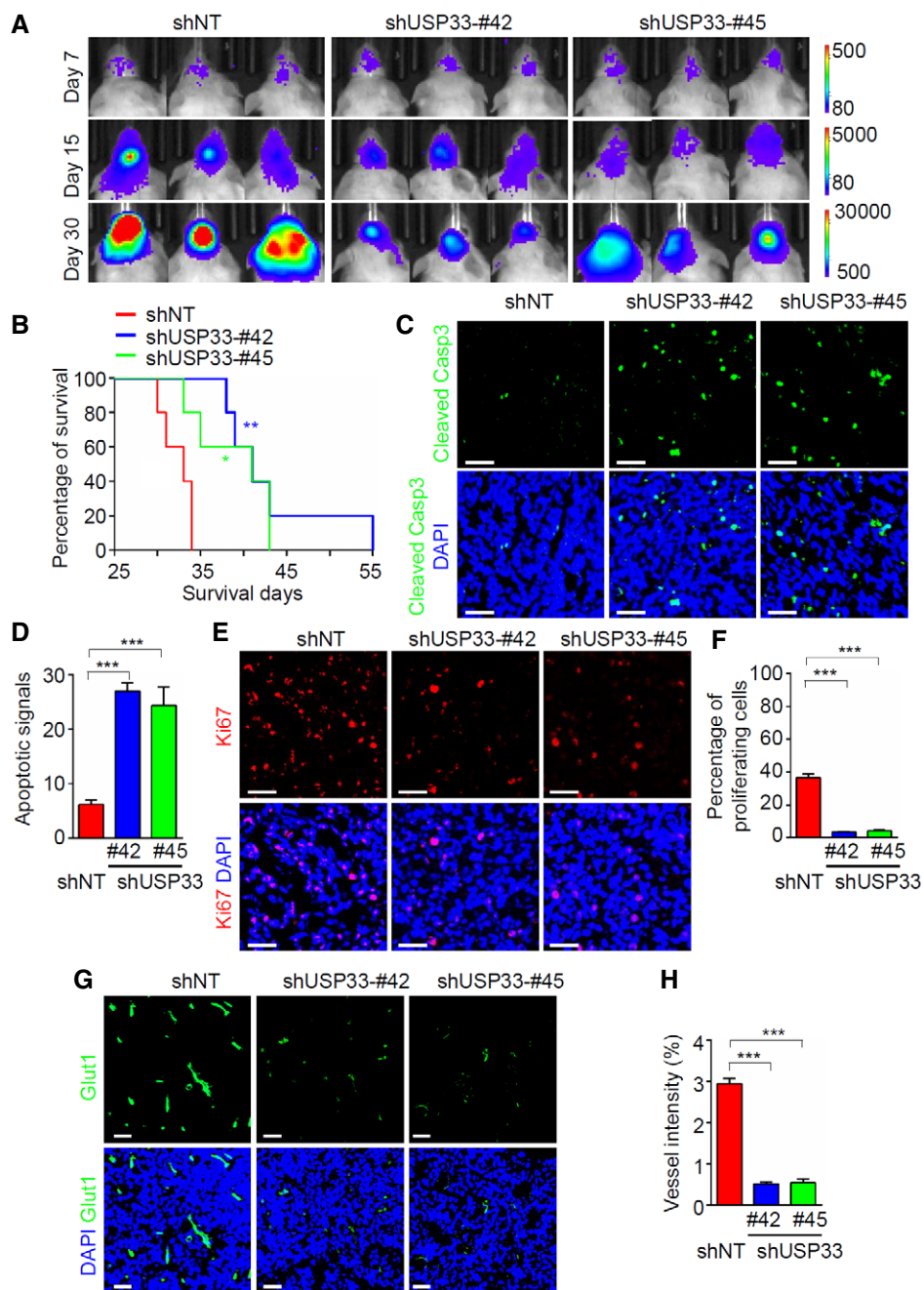
Figure 7. Disrupting USP33 inhibited growth of GSC-derived GBM xenografts.

A   *In vivo* bioluminescent imaging analysis of intracranial tumor growth in mice bearing GBM xenografts derived from the T387 GSCs expressing shUSP33 or shNT. Two-thousand GSCs transduced with luciferase and shUSP33 or shNT were implanted into mouse brains through intracranial injection. Representative bioluminescent images on day 7, day 15, and day 30 post-transplantation of GSCs were shown. Disruption of USP33 delayed tumor growth of intracranial GBM xenografts.

B   Kaplan–Meier survival curves of mice bearing GBMs derived from T387 GSCs expressing shUSP33 or shNT from (A). Disruption of USP33 extended the survival of mice bearing GSC-derived GBM tumors. ($n = 5$ mice for each group; shUSP33#42 vs. shNT, $P = 0.0185$; shUSP33#45 vs. shNT, $P = 0.0027$; two-tailed log-rank test).

C, D   Immunofluorescent analysis (C) and statistical quantifications (D) of the apoptotic marker cleaved caspase-3 in xenografts derived from T387 GSCs expressing shUSP33 or shNT. Disruption of USP33 in GSCs dramatically elevated apoptosis in GBM tumors. Scale bar, 80 μm. ($n = 5$ tumors for each group; ***$P < 0.001$; mean ± s.e.m.; two-tailed unpaired *t*-test).

E, F   Immunofluorescent analysis (E) and statistical quantifications (F) of the cell proliferation marker Ki67 in xenografts derived from T387 GSCs expressing shUSP33 or shNT. Disruption of USP33 in GSCs reduced cell proliferation in GBM xenografts. Scale bar, 80 μm. ($n = 5$ tumors for each group; ***$P < 0.001$; mean ± s.e.m.; two-tailed unpaired *t*-test).

G, H   Immunofluorescent analysis (G) and statistical quantifications (H) of the vascular endothelial cell marker Glut1 in xenografts derived from T387 GSCs expressing shUSP33 or shNT. Disruption of USP33 in GSCs reduced vessel intensity in GBM xenografts. Scale bar, 80 μm. ($n = 5$ tumors for each group; ***$P < 0.001$; mean ± s.e.m.; two-tailed unpaired *t*-test).

hypoxic conditions. Despite the similarities between HIF1α and HIF2α, USP33 did not interact with HIF1α (Appendix Fig S8A). Over-expression or disruption of USP33 in GSCs showed negligible effects on HIF1α protein levels (Appendix Fig S8B–D). Therefore, the discovery of USP33 as a hypoxia-inducible DUB specifically for HIF2α in GSCs highlights the sophisticated molecular mechanisms controlling the oxygen-dependent regulation of different HIFs.

USP33 is also named as the VHL-interacting deubiquitinating enzyme 1 (VDU1), which shares an approximately 59% identity with USP20/VDU2 (Li *et al*, 2002). Both USP33 and USP20 interact with VHL, but hypoxia induces the interaction between USP20 and HIF1α to deubiquitinate and stabilize HIF1α, whereas USP33 shows no affinity to HIF1α (Li *et al*, 2005). Little is known about the substrates and functions of USP33. It has been reported that USP33 deubiquitinates the Robo-1 receptor and promotes Slit/Robo signaling in regulating neuronal axon guidance and tumor cell migration (Yuasa-Kawada *et al*, 2009). In addition, USP33 deubiquitinates the centriolar protein CP110 that is essential for centrosome amplification (Li *et al*, 2013). In this study, we discovered that USP33 is induced by hypoxia preferentially in GSCs to deubiquitinate and stabilize HIF2α, promoting the maintenance of GSCs. The molecular mechanisms driving the upregulation of USP33 in GSCs in response to hypoxia remain to be further investigated. We found no change in the transcription of USP33 in response to hypoxia (Appendix Fig S9A). Disruption of neither HIF1α nor HIF2α affected USP33 protein levels under hypoxic conditions (Appendix Fig S9B and C), suggesting that the hypoxia induction of USP33 is not under the control of HIFs. Because USP33 is a VHL-interacting protein, the protein stability of USP33 may be affected by the VHL-mediated ubiquitin–proteasomal degradation. Nevertheless, USP33 lacks the oxygen-dependent degradation domains or the conserved hydroxylation motif LXXLAP that mediates the oxygen-sensitive binding of VHL (Huang *et al*, 1998; Masson *et al*, 2001). Moreover, biochemical studies showed that the 91-113aa region in the VHL protein mediates its interaction with HIFs, but the 54-83aa region is responsible for the USP33 binding (Tanimoto *et al*, 2000; Li *et al*, 2002). Therefore, the hypoxia-responsive regulation of USP33 may not simply resemble the stabilization of HIFs by hypoxia-induced dissociation of VHL. Recent studies showed that USP33 may be degraded by another E3 enzyme HERC2 (Chan *et al*, 2014). USP33 and HERC2 were in a complex containing p97 and NPL4/UFD1, which recapitulates the formation of the complex consisting of HIF1α, VHL, p97, and NPL4/UFD1 under normoxia that mediates HIF1α degradation (Alexandru *et al*, 2008; Chan *et al*, 2014). In addition, depletion of p97 resulted in accumulation of HIF1α and USP33 (Alexandru *et al*, 2008; Chan *et al*, 2014). It would be interesting to study whether USP33 is in the oxygen-sensitive protein complex containing HERC2 or VHL that may regulate the induction of USP33 under hypoxia.

Hypoxia-inducible factors proteins are functionally regulated through multiple post-translational modifications including hydroxylation, phosphorylation, acetylation, sumoylation, and methylation (Keith *et al*, 2011). Although phosphorylation of HIF2α has been noticed for a while, little is known about the catalytic enzymes and the functions. In this study, we found that activated ERK1/2 phosphorylate S484 on human HIF2α to promote the interaction between HIF2α and USP33, resulting in HIF2α stabilization and accumulation in GSCs in response to hypoxia. Numerous reports have demonstrated the activation of ERK1/2 in response to hypoxia. Hypoxia-induced ERK1/2 may be under the control of VHL. VHL binds to and degrades the hydroxylated NDRG3 protein under normoxia, whereas hypoxia stabilizes NDRG3 that binds to c-Raf and activates the c-Raf-ERK1/2 pathway (Stalmans *et al*, 2015). Although our study showed that ERK1/2 were the upstream regulators of HIF2α, other studies reported that ERK1/2 may also be regulated by HIF2α (Ramakrishnan *et al*, 2016). However, disruption of neither HIF1α nor HIF2α altered ERK1/2 activation in GSCs in response to hypoxia (Appendix Fig S9B and C). In fact, phosphorylation of ERK1/2 occurred ahead of HIF2α upregulation in response to hypoxia in GSCs (Appendix Fig S9D). Thus, hypoxia-induced activation of ERK1/2 may be independent of HIFs at least in GSCs. HIF2α holds multiple potential phosphorylation sites for ERK1/2, including S484, S581, and S672. Our data showed that the S484 phosphorylation was critical for the interaction between HIF2α and USP33 (Fig 6F and G). Previous reports showed that S672 mediated the interaction between HIF2α and CRM1 (chromosomal maintenance 1) to affect the localization but not stability of HIF2α protein (Gkotinakou *et al*, 2019). Interestingly, both S484 and S581 are localized within the N-terminal TAD (transactivation domain) that determines the target gene specificity of HIF2α. Replacement of the N-TAD of HIF2α with the analogous region of HIF1α will convert HIF2α into a protein with HIF1α functional specificity (Hu *et al*, 2007). It is possible that the phosphorylation sites within the N-TAD may determine the selective binding of HIF2α to USP33. In addition, S484 is in the ODD domain of HIF2α and is flanked by the two critical hydroxylation sites P405 and P531 (Keith *et al*, 2011). Thus, the ODD of HIF2α may function as an oxygen-sensitive molecular switch through binding to the ubiquitin E3 ligase VHL under normoxia and promoting interaction with the deubiquitinase USP33 under hypoxia.

In summary, our findings highlight USP33 as a critical hypoxia-inducible DUB that deubiquitinates and stabilizes HIF2α in response to hypoxia to promote GSC maintenance and GBM tumor growth. Activation of ERK1/2 upon hypoxia is able to phosphorylate HIF2α at S484 to promote the interaction between USP33 and HIF2α, which reduces HIF2α ubiquitination to stabilize this critical protein. Our findings not only uncover the key DUB responsible for HIF2α stabilization and GSC adaption to hypoxia but also provide new insight into the function of ERK1/2 activity in hypoxia response. These discoveries may be utilized to develop new therapeutic strategies to target GSCs in the hypoxic tumor microenvironment to improve GBM treatment.

Materials and Methods

Human GBM specimens, glioma stem cells (GSCs), and non-stem tumor cells (NSTCs)

Deidentified GBM surgical specimens were collected from The Brain Tumor and Neuro-Oncology Center at Cleveland Clinic in accordance with an Institutional Review Board-approved protocol. Informed consent was obtained from all subjects. GSCs and matched non-stem tumor cells (NSTCs) were isolated from primary GBMs or xenografts and cultured as previously described (Bao *et al*, 2006; Zhou *et al*, 2017). In brief, glioma cells were isolated from GBM tumors with Papain Dissociation System (Worthington Biochemical, LK003153). After recovery in the stem cell medium (Neurobasal-A

medium (Thermo Fisher, A2477501) with B27 supplement (Thermo Fisher, 12587010), 10 ng/ml EGF (Gold biotechnology, 1150-04-1000), 10 ng/ml bFGF (R&D Systems, 4114-TC-01 M), 2 mM L-glutamine (Thermo Fisher, 35050061), and 1 mM sodium pyruvate (Thermo Fisher, 11360070)) for at least 6 h for the reexpression of surface markers, the isolated cells were then labeled with a phycoerythrin (PE)-conjugated anti-CD133 antibody (Miltenyi Biotec, 130-098-826) and a FITC-conjugated anti-CD15 antibody (Millipore, CBL144F) followed by fluorescence-activated cell sorting (FACS) to sort the GSC population (CD15$^+$/CD133$^+$) and the NSTC population (CD15$^-$/CD133$^-$). A series of functional assays were then applied to validate the cancer stem cell phenotypes of the isolated GSCs, including self-renewal (serial neurosphere formation), multipotent differentiation (induction of multi-lineage differentiation *in vitro*), and tumor initiation (*in vivo* limiting dilution assay) as previously described (Bao *et al*, 2006; Zhou *et al*, 2017). The validated GSCs were then used for further experiments. GSCs were cultured in the stem cell medium, and NSTCs were cultured in DMEM with 10% FBS to maintain differentiation status. For western blots, the DMEM medium for NSTC was changed to the stem cell medium 12 h before harvest to avoid potential bias from different cell culture systems.

Intracranial tumor formation

Intracranial transplantation of GSCs to establish orthotopic GBM xenografts was performed as described (Bao *et al*, 2006; Zhou *et al*, 2017). GSCs were infected with indicated shRNAs and/or with luciferase through lentiviral infection. Cells were selected with puromycin (1 μg/ml, Fisher Scientific) for 48 h after infection. A total of 2,000 cells were then engrafted intracranially into immunocompromised NSG mice (Jackson Laboratories, 005557, or the Cleveland Clinic's Biological Resources Unit) into the right cerebral cortex at a depth of 2.5–3.5 mm. Animals were monitored by bioluminescent imaging or maintained until manifestation of neurological signs. For *in vivo* bioluminescent imaging, firefly luciferase was transduced into GSCs through lentiviral infection followed by two rounds of puromycin selection. Mice bearing GSC-derived xenografts were injected with D-luciferin (Goldbio, LUCK-1G) at 150 mg/kg intratoneally and the bioluminescent signals reflecting tumor growth were captured by Spectrum IVIS imaging system (PerkinElmer). All animal protocols were approved by the Animal Research Committee of the Cleveland Clinic, and all animals were housed in the Association for the Assessment and Accreditation of Laboratory Animal Care-accredited animal facility at Cleveland Clinic Lerner Research Institute. No specific method was used to predetermine sample size. The experiments were not randomized. Only animals with accidental death (e.g., due to infection or intracranial injection) were excluded from the data analysis. The investigators were not blinded to allocation during experiments and outcome assessment.

Immunofluorescent staining and *in vivo* labeling of hypoxic cells

Immunofluorescent staining was performed as described before (Zhou *et al*, 2017; Zhang *et al*, 2020). Surgical human GBM specimens or intracranial xenografts were fixed overnight in 4% PFA at 4°C, stored in 30% sucrose solution overnight at 4°C, embedded in OCT at −20°C overnight, and cryosectioned at a thickness of 8 μm. Sections were blocked with a PBS solution containing 1% BSA (Sigma) plus 0.03% TWEEN-20 for 1 h at room temperature and incubated with primary antibodies (1:200 dilution) overnight at 4°C. After then, the sections were washed with a cold PBS solution containing 1% BSA (Sigma) plus 0.03% TWEEN-20 and incubated with secondary antibodies (1:200 dilution) for 2 h followed by DAPI for 5 min at room temperature and then subjected to microscopy. Specific antibodies against the hypoxia marker CA9 (Novus, NBP1-51691 or NB100-417), the GSC markers GSC marker SOX2 (Millipore AB5603; Santa Cruz sc-17320) or Olig2 (R&D systems AF2418), HIF1α (Novus, NB100-449), HIF2α (Novus, NB100-122), USP33 (Novus, H00023032-M01 or Bethyl, A300-925A), the cell apoptotic marker cleaved caspase-3 (Cell Signaling Tech. 9661), the cell proliferation marker Ki67 (Abcam, ab15580), the astrocyte marker GFAP (Biolegend, 840001), the neuronal marker TUJ1 (Biolegend, 801202), and the endothelial cell markers Glut1 (Thermo Fisher, RB-9052-P) and CD34 (Biolegend, 343502) were used for the staining on GBM tumor sections as indicated. Glut1-positive areas were regarded as vessels and determined by ImageJ.

In vivo labeling of the hypoxic cells was carried with the Hypoxyprobe Plus kit (Hypoxyprobe Inc., HP2-100Kit) according to the manufacturer's instructions. Briefly, mice bearing intracranial xenografts were injected intravenously (tail vein) with 60 mg/kg of pimonidazole and were sacrificed 2 h post-injection. Intracranial GBM xenografts were fixed in 4% PFA at 4°C overnight, stored in 30% sucrose solution overnight at 4°C, embedded in OCT at −20°C overnight, and cryosectioned at a thickness of 8 μm. Pimonidazole is reductively activated in hypoxic cells and forms stable adducts with thiol (sulphydryl) groups in proteins, peptides, and amino acids. Therefore, the hypoxic cells were stained with the FITC-conjugated IgG1 monoclonal anti-pimonidazole antibody (MAb clone 4.3.11.3).

TUNEL assay

TUNEL assays detecting apoptosis in tumor sections were performed with a Click-iT™ Plus TUNEL Assay kit (Invitrogen, C10618) according to manufacturer's instructions. In brief, sections were incubated with Proteinase K working solution in a humidified chamber at room temperature for 15 min and then washed with PBS. The sections were then incubated in 4% PFA in PBS at 37°C for 15 min, washed with PBS, and rinsed with ddH$_2$O. After incubation in TdT Reaction Buffer at 37°C for 10 min, the sections were incubated in the TdT reaction mixture in a humidified chamber at 37°C for 60 min. The sections were then rinsed with ddH$_2$O, incubated in 3% BSA and 0.1% Triton™ X-100 in PBS for 5 min, and rinsed with PBS. The samples were then completely immersed in the Click-iT™ Plus TUNEL Reaction cocktail and incubated for 30 min at 37°C in dark. After then, the sections were washed with 3% BSA in PBS for 5 min, rinsed with PBS, stained with Hoechst for 15 min, washed with PBS, and then subjected to microscopy.

Cell viability and *in vitro* limiting dilution assay

For cell viability assay, 2,000 cells (for GSCs) or 5,000 cells (NSTCs) per well were plated in a 96-well plate. Viable cells at different time points were measured using the Cell Titer-Glo Luminescent Cell Viability Assay kit (Promega, G7571) according to the manufacturer's instructions. For *in vitro* limiting dilution assay, cells were

infected with lentiviruses and recovered for 15 days. GSC tumorspheres were dissociated for subculture twice a week. At the starting point of experiment, different numbers of GSCs (0, 4, 8, 12, and 16 cells/well) were seeded into 96-well plates, each cell density with 24 replicates. The numbers of wells with the presence of neurospheres were recorded at Day 5 post-seeding, and the clonogenic ability of cells was analyzed using the software at: http://bioinf.wehi.edu.au/software/elda/.

Plasmid constructs and lentivirus production

The 4HRE-d2GFP reporter was constructed by replacing the CMV promoter of the pCDH-CMV-MCS-EF1-Puro vector (System Biosciences CD510B-1) with an insert of four repetitive cis-acting hypoxia-responsive elements (HRE) from the VEGF promoter followed by a minimum CMV promoter, which was subcloned from the 5HRE-GFP plasmid purchased from Addgene (Plasmid 46926) (Vordermark et al, 2001). The wild-type and catalytically dead USP33 in pEGFP-C1 vector were kind gifts from Dr. Michael J. Clague (University of Liverpool, UK) (Thorne et al, 2011), which were later subcloned into the pCDH-CMV-MCS-EF1-Puro vector for lentivirus package. The wild-type and hydroxylation mutated 2dPA HIF2α in pcDNA3 vector were purchased from Addgene (Plasmid 18950 and 18956; Kondo et al, 2002; Yan et al, 2007) and subcloned into pRLenti-CMV-PGK-Puro vector for lentivirus package. The S484A, S581A, and S672A HIF2α mutants were generated with the QuikChange® II XL Site-Directed Mutagenesis kit (Agilent, 200522) according to the manufacturer's instruction. shRNAs targeting USP33 (SHCLNG-NM_015017, TRCN0000004442, and TRCN0000004445), HIF1α (SHCLNG- NM_001530, TRCN0000003809, and TRCN0000003810), HIF2α (SHCLNG-NM_001430, TRCN0000003803, and TRCN0000003804), or the shNT control shRNA (SHC002) were purchased from Sigma. For lentivirus production, 293FT cells were transfected with the desired plasmid together with the helper plasmids pCI-VSVG and ps-PAX2. After 48–72 h transfection, lentiviral supernatant was collected and tittered as described previously (Zhou et al, 2017; Zhang et al, 2020). GSCs were then infected with lentivirus at a MOI around 3.

Immunoblot analysis and immunoprecipitation

Immunoblotting was performed as previously described (Zhang et al, 2020). Briefly, cells were lysed in TritonX-100 lysis buffer (1% TritonX-100, 10% glycerol, 50 mM HEPES pH7.5, 150 mM NaCl, 100 mM NaF, 1 mM PMSF, 1 mM Na3VO4, and protease inhibitor cocktail) and subjected to SDS-PAGE. After SDS-PAGE, proteins were transferred to PVDF membrane (Biorad), blocked by 5% milk for 30 min, and incubated with primary antibody overnight at 4°C. Membranes were washed with TBST for three times and incubated with secondary antibody for 2 h at room temperature. Membranes were then washed with TBST for three times and subjected to chemiluminescent substrate (Thermo Scientific). Signals were detected with ChemiDoc XRS⁺ Imager (Biorad).

For immunoprecipitation, cells were lysed in TritonX-100 lysis buffer and centrifuged at 15,000 g for 10 min. Supernatant cell lysates of approximately 200–400 µg total proteins were incubated with 20 µl of Protein A/G agarose gel (Santa Cruz, sc-2003) along with primary antibodies against HIF2α (Novus, NB100-122) or

USP33 (Novus, H00023032-M01), normal mouse IgG (Santa Cruz, sc-2025) or normal rabbit IgG (Cell Signaling, 2729). Anti-HA-agarose (Sigma, A2095) was used for immunoprecipitation of HA-tagged proteins. The immunoprecipitation system was adjusted to a volume of 1 ml by addition of cold PBS supplemented with 0.3% Triton X-100, and then the mixture was subjected to constant rotation at 80 rpm overnight at 4°C. Immunocomplexes were washed three times with ice-cold 0.3% Triton X-100 in PBS buffer and eluted in loading buffer by boiling for 10 min, and then analyzed by immunoblotting. For co-immunoprecipitation, half of the immunoprecipitation product was used for immunoblot of the prey, while the other half was used for the bait protein. Proteins were resolved on NuPAGE Novex 4–12% Bis-Tris gels (Invitrogen, NP0322BOX), blotted onto PVDF membranes and probed by indicated antibodies.

Specific antibodies against HIF1α (Novus, NB100-449), HIF2α (Novus, NB100-122), USP33 (Novus, H00023032-M01), USP1 (Abcam, ab108104), USP7 (Abcam, ab119364), USP10 (Cell Signaling Technology, 8501), USP8 (Bethyl, A302-929A), USP13 (Abcam, ab109264), USP14 (Thermo, PA5-12015), USP19 (Abcam, ab68527), USP20 (Abcam, ab119918), USP28 (Abcam, ab126604), USP31 (Abcam, ab57451), USP34 (Bethyl, A300-824A), USP36 (Santa Cruz, sc-82102), USP47(Santa Cruz, sc-100633), HA (Sigma, 11867423001), GFP (Santa Cruz, sc-8334), tubulin (Sigma, T6199), Flag (Sigma, F1804), ERK1/2 (Biolegend, 686902), pERK1/2 (Cell Signaling Technology, 4370), ubiquitin (Biolegend, 646302), and pS/T (BD Biosciences, 612548) were used for immunoblot.

Ubiquitination assay

The ubiquitination assay was performed as previously described (Huang et al, 2011). Cells were treated with 20 µM MG132 for 6 h before harvest. Cell lysate was subjected to immunoprecipitation and the product was eluted in loading buffer by boiling for 10 min. Proteins were resolved on NuPAGE Novex 4–12% Bis-Tris gels (Invitrogen, NP0322BOX), blotted onto PVDF membranes and probed by the anti-ubiquitin antibody.

Quantitative PCR

Total RNA was isolated with the PureLink RNA mini extraction kit (Thermo Fisher, 12183018A), reverse transcribed with the PrimeScript RT Reagent kit (Takara, RR037A), and analyzed by quantitative PCR using SYBR Green (Alkali Scientific, QS2050) and the ABI 7500 system (Applied Biosystems). Cycle threshold (Ct) values were determined automatically by the ABI 7500 system. At least three biological repeats were performed for each analysis, whereas a representative result containing three technical replicates were used to generate graphs. The primers for qPCR analysis are included in the Appendix Table S1.

Quantification and statistical analysis

The level of significance was determined by the unpaired two-tailed Student's t-test (bar graphs) or two-tailed log-rank test with α = 0.05 (Kaplan–Meier survival curves) with the GraphPad Prism 5 software. All quantitative data presented are the mean ± s.e.m. from at least three samples or experiments per data point. Precise

experimental details (number of animals or cells and experimental replication) are provided in the figure legends.

Data availability

This study includes no data deposited in external repositories.

Expanded View for this article is available online.

Acknowledgements

Author contributions

Disclosure and competing interests statement

The authors declare that they have no conflict of interest.

References

Alexandru G, Graumann J, Smith GT, Kolawa NJ, Fang R, Deshaies RJ (2008) UBXD7 binds multiple ubiquitin ligases and implicates p97 in HIF1alpha turnover. *Cell* 134: 804–816

Altun M, Zhao B, Velasco K, Liu H, Hassink G, Paschke J, Pereira T, Lindsten K (2012) Ubiquitin-specific protease 19 (USP19) regulates hypoxia-inducible factor 1alpha (HIF-1alpha) during hypoxia. *J Biol Chem* 287: 1962–1969

Bao S, Wu Q, McLendon RE, Hao Y, Shi Q, Hjelmeland AB, Dewhirst MW, Bigner DD, Rich JN (2006) Glioma stem cells promote radioresistance by preferential activation of the DNA damage response. *Nature* 444: 756–760

Berthouze M, Venkataramanan V, Li Y, Shenoy SK (2009) The deubiquitinases USP33 and USP20 coordinate beta2 adrenergic receptor recycling and resensitization. *EMBO J* 28: 1684–1696

Bett JS, Ibrahim AF, Garg AK, Kelly V, Pedrioli P, Rocha S, Hay RT (2013) The P-body component USP52/PAN2 is a novel regulator of HIF1A mRNA stability. *Biochem J* 451: 185–194

Birner P, Schindl M, Obermair A, Plank C, Breitenecker G, Oberhuber G (2000) Overexpression of hypoxia-inducible factor 1alpha is a marker for an unfavorable prognosis in early-stage invasive cervical cancer. *Cancer Res* 60: 4693–4696

Branco-Price C, Zhang N, Schnelle M, Evans C, Katschinski DM, Liao D, Ellies L, Johnson RS (2012) Endothelial cell HIF-1alpha and HIF-2alpha differentially regulate metastatic success. *Cancer Cell* 21: 52–65

Bremm A, Moniz S, Mader J, Rocha S, Komander D (2014) Cezanne (OTUD7B) regulates HIF-1alpha homeostasis in a proteasome-independent manner. *EMBO Rep* 15: 1268–1277

Chan NC, den Besten W, Sweredoski MJ, Hess S, Deshaies RJ, Chan DC (2014) Degradation of the deubiquitinating enzyme USP33 is mediated by p97 and the ubiquitin ligase HERC2. *J Biol Chem* 289: 19789–19798

Choi YK, Kim CK, Lee H, Jeoung D, Ha KS, Kwon YG, Kim KW, Kim YM (2010) Carbon monoxide promotes VEGF expression by increasing HIF-1alpha protein level via two distinct mechanisms, translational activation and stabilization of HIF-1alpha protein. *J Biol Chem* 285: 32116–32125

Clague MJ, Urbe S, Komander D (2019) Breaking the chains: deubiquitylating enzyme specificity begets function. *Nat Rev Mol Cell Biol* 20: 338–352

Conrad PW, Freeman TL, Beitner-Johnson D, Millhorn DE (1999) EPAS1 trans-activation during hypoxia requires p42/p44 MAPK. *J Biol Chem* 274: 33709–33713

Doe MR, Ascano JM, Kaur M, Cole MD (2012) Myc posttranscriptionally induces HIF1 protein and target gene expression in normal and cancer cells. *Cancer Res* 72: 949–957

Doeppner TR, Doehring M, Bretschneider E, Zechariah A, Kaltwasser B, Muller B, Koch JC, Bahr M, Hermann DM, Michel U (2013) MicroRNA-124 protects against focal cerebral ischemia via mechanisms involving Usp14-dependent REST degradation. *Acta Neuropathol* 126: 251–265

Fan Y, Potdar AA, Gong Y, Eswarappa SM, Donnola S, Lathia JD, Hambardzumyan D, Rich JN, Fox PL (2014) Profilin-1 phosphorylation directs angiocrine expression and glioblastoma progression through HIF-1alpha accumulation. *Nat Cell Biol* 16: 445–456

Fang X, Zhou W, Wu Q, Huang Z, Shi YU, Yang K, Chen C, Xie QI, Mack SC, Wang X *et al* (2017) Deubiquitinase USP13 maintains glioblastoma stem cells by antagonizing FBXL14-mediated Myc ubiquitination. *J Exp Med* 214: 245–267

Faronato M, Patel V, Darling S, Dearden L, Clague MJ, Urbe S, Coulson JM (2013) The deubiquitylase USP15 stabilizes newly synthesized REST and rescues its expression at mitotic exit. *Cell Cycle* 12: 1964–1977

Fluegen G, Avivar-Valderas A, Wang Y, Padgen MR, Williams JK, Nobre A, Calvo V, Cheung JF, Bravo-Cordero JJ, Entenberg D *et al* (2017) Phenotypic heterogeneity of disseminated tumour cells is preset by primary tumour hypoxic microenvironments. *Nat Cell Biol* 19: 120–132

Flugel D, Gorlach A, Kietzmann T (2012) GSK-3beta regulates cell growth, migration, and angiogenesis via Fbw7 and USP28-dependent degradation of HIF-1alpha. *Blood* 119: 1292–1301

Forsythe JA, Jiang BH, Iyer NV, Agani F, Leung SW, Koos RD, Semenza GL (1996) Activation of vascular endothelial growth factor gene transcription by hypoxia-inducible factor 1. *Mol Cell Biol* 16: 4604–4613

Franovic A, Holterman CE, Payette J, Lee S (2009) Human cancers converge at the HIF-2alpha oncogenic axis. *Proc Natl Acad Sci USA* 106: 21306–21311

Giatromanolaki A, Koukourakis MI, Sivridis E, Turley H, Talks K, Pezzella F, Gatter KC, Harris AL (2001) Relation of hypoxia inducible factor 1 alpha and 2 alpha in operable non-small cell lung cancer to

angiogenic/molecular profile of tumours and survival. *Br J Cancer* 85: 881–890

Gkotinakou IM, Befani C, Simos G, Liakos P (2019) ERK1/2 phosphorylates HIF-2alpha and regulates its activity by controlling its CRM1-dependent nuclear shuttling. *J Cell Sci* 132: jcs225698

Gonzalez FA, Raden DL, Davis RJ (1991) Identification of substrate recognition determinants for human ERK1 and ERK2 protein kinases. *J Biol Chem* 266: 22159–22163

Goto Y, Zeng L, Yeom CJ, Zhu Y, Moribu A, Shinomiya K, Kobayashi M, Hirota K, Itasaka S, Yoshimura M *et al* (2015) UCHL1 provides diagnostic and antimetastatic strategies due to its deubiquitinating effect on HIF-1alpha. *Nat Commun* 6: 6153

Helczynska K, Larsson AM, Holmquist Mengelbier L, Bridges E, Fredlund E, Borgquist S, Landberg G, Pahlman S, Jirstrom K (2008) Hypoxia-inducible factor-2alpha correlates to distant recurrence and poor outcome in invasive breast cancer. *Cancer Res* 68: 9212–9220

Holmquist-Mengelbier L, Fredlund E, Lofstedt T, Noguera R, Navarro S, Nilsson H, Pietras A, Vallon-Christersson J, Borg A, Gradin K *et al* (2006) Recruitment of HIF-1alpha and HIF-2alpha to common target genes is differentially regulated in neuroblastoma: HIF-2alpha promotes an aggressive phenotype. *Cancer Cell* 10: 413–423

Hu CJ, Sataur A, Wang L, Chen H, Simon MC (2007) The N-terminal transactivation domain confers target gene specificity of hypoxia-inducible factors HIF-1alpha and HIF-2alpha. *Mol Biol Cell* 18: 4528–4542

Hu CJ, Wang LY, Chodosh LA, Keith B, Simon MC (2003) Differential roles of hypoxia-inducible factor 1alpha (HIF-1alpha) and HIF-2alpha in hypoxic gene regulation. *Mol Cell Biol* 23: 9361–9374

Huang LE, Gu J, Schau M, Bunn HF (1998) Regulation of hypoxia-inducible factor 1alpha is mediated by an O2-dependent degradation domain via the ubiquitin-proteasome pathway. *Proc Natl Acad Sci USA* 95: 7987–7992

Huang Z, Wu Q, Guryanova OA, Cheng L, Shou W, Rich JN, Bao S (2011) Deubiquitylase HAUSP stabilizes REST and promotes maintenance of neural progenitor cells. *Nat Cell Biol* 13: 142–152

Kaelin Jr WG, Ratcliffe PJ (2008) Oxygen sensing by metazoans: the central role of the HIF hydroxylase pathway. *Mol Cell* 30: 393–402

Keith B, Johnson RS, Simon MC (2011) HIF1alpha and HIF2alpha: sibling rivalry in hypoxic tumour growth and progression. *Nat Rev Cancer* 12: 9–22

Kim D, Hong A, Park HI, Shin WH, Yoo L, Jeon SJ, Chung KC (2017) Deubiquitinating enzyme USP22 positively regulates c-Myc stability and tumorigenic activity in mammalian and breast cancer cells. *J Cell Physiol* 232: 3664–3676

Klatte T, Seligson DB, Riggs SB, Leppert JT, Berkman MK, Kleid MD, Yu H, Kabbinavar FF, Pantuck AJ, Belldegrun AS (2007) Hypoxia-inducible factor 1 alpha in clear cell renal cell carcinoma. *Clin Cancer Res* 13: 7388–7393

Kokate SB, Dixit P, Das L, Rath S, Roy AD, Poirah I, Chakraborty D, Rout N, Singh SP, Bhattacharyya A (2018) Acetylation-mediated Siah2 stabilization enhances PHD3 degradation in *Helicobacter pylori*-infected *gastric epithelial cancer cells*. *FASEB J* 32: 5378–5389

Kondo K, Klco J, Nakamura E, Lechpammer M, Kaelin Jr WG (2002) Inhibition of HIF is necessary for tumor suppression by the von Hippel-Lindau protein. *Cancer Cell* 1: 237–246

LaGory EL, Giaccia AJ (2016) The ever-expanding role of HIF in tumour and stromal biology. *Nat Cell Biol* 18: 356–365

Lee D, Sohn H, Park Z-Y, Oh S, Kang Y, Lee K-M, Kang M, Jang Y, Yang S-J, Hong Y *et al* (2015) A lactate-induced response to hypoxia. *Cell* 161: 595–609

Lee SB, Frattini V, Bansal M, Castano AM, Sherman D, Hutchinson K, Bruce JN, Califano A, Liu G, Cardozo T *et al* (2016) An ID2-dependent mechanism for VHL inactivation in cancer. *Nature* 529: 172–177

Li J, D'Angiolella V, Seeley ES, Kim S, Kobayashi T, Fu W, Campos EI, Pagano M, Dynlacht BD (2013) USP33 regulates centrosome biogenesis via deubiquitination of the centriolar protein CP110. *Nature* 495: 255–259

Li J, Xu Y, Long XD, Wang W, Jiao HK, Mei Z, Yin QQ, Ma LN, Zhou AW, Wang LS *et al* (2014) Cbx4 governs HIF-1alpha to potentiate angiogenesis of hepatocellular carcinoma by its SUMO E3 ligase activity. *Cancer Cell* 25: 118–131

Li L, Xiong Y, Qu Y, Mao M, Mu W, Wang H, Mu D (2008) The requirement of extracellular signal-related protein kinase pathway in the activation of hypoxia inducible factor 1 alpha in the developing rat brain after hypoxia-ischemia. *Acta Neuropathol* 115: 297–303

Li Z, Bao S, Wu Q, Wang H, Eyler C, Sathornsumetee S, Shi Q, Cao Y, Lathia J, McLendon RE *et al* (2009) Hypoxia-inducible factors regulate tumorigenic capacity of glioma stem cells. *Cancer Cell* 15: 501–513

Li Z, Na X, Wang D, Schoen SR, Messing EM, Wu G (2002) Ubiquitination of a novel deubiquitinating enzyme requires direct binding to von Hippel-Lindau tumor suppressor protein. *J Biol Chem* 277: 4656–4662

Li Z, Wang D, Messing EM, Wu G (2005) VHL protein-interacting deubiquitinating enzyme 2 deubiquitinates and stabilizes HIF-1alpha. *EMBO Rep* 6: 373–378

Loenarz C, Coleman ML, Boleininger A, Schierwater B, Holland PW, Ratcliffe PJ, Schofield CJ (2011) The hypoxia-inducible transcription factor pathway regulates oxygen sensing in the simplest animal, *Trichoplax adhaerens*. *EMBO Rep* 12: 63–70

Ma L, Hernandez MO, Zhao Y, Mehta M, Tran B, Kelly M, Rae Z, Hernandez JM, Davis JL, Martin SP *et al* (2019) Tumor cell biodiversity drives microenvironmental reprogramming in liver cancer. *Cancer Cell* 36: 418–430

Man J, Yu X, Huang H, Zhou W, Xiang C, Huang H, Miele L, Liu Z, Bebek G, Bao S *et al* (2018) Hypoxic induction of vasorin regulates notch1 turnover to maintain glioma stem-like cells. *Cell Stem Cell* 22: 104–118

Masson N, Keeley TP, Giuntoli B, White MD, Puerta ML, Perata P, Hopkinson RJ, Flashman E, Licausi F, Ratcliffe PJ (2019) Conserved N-terminal cysteine dioxygenases transduce responses to hypoxia in animals and plants. *Science* 365: 65–69

Masson N, Willam C, Maxwell PH, Pugh CW, Ratcliffe PJ (2001) Independent function of two destruction domains in hypoxia-inducible factor-alpha chains activated by prolyl hydroxylation. *EMBO J* 20: 5197–5206

Mennerich D, Kubaichuk K, Kietzmann T (2019) DUBs, hypoxia, and cancer. *Trends Cancer* 5: 632–653

Minet E, Arnould T, Michel G, Roland I, Mottet D, Raes M, Remacle J, Michiels C (2000) ERK activation upon hypoxia: involvement in HIF-1 activation. *FEBS Lett* 468: 53–58

Moniz S, Bandarra D, Biddlestone J, Campbell KJ, Komander D, Bremm A, Rocha S (2015) Cezanne regulates E2F1-dependent HIF2alpha expression. *J Cell Sci* 128: 3082–3093

Mukhopadhyay D, Tsiokas L, Zhou XM, Foster D, Brugge JS, Sukhatme VP (1995) Hypoxic induction of human vascular endothelial growth factor expression through c-Src activation. *Nature* 375: 577–581

Niu K, Fang H, Chen Z, Zhu Y, Tan Q, Wei D, Li Y, Balajee AS, Zhao Y (2020) USP33 deubiquitinates PRKN/parkin and antagonizes its role in mitophagy. *Autophagy* 16: 724–734

Osada R, Horiuchi A, Kikuchi N, Yoshida J, Hayashi A, Ota M, Katsuyama Y, Melillo G, Konishi I (2007) Expression of hypoxia-inducible factor 1alpha, hypoxia-inducible factor 2alpha, and von Hippel-Lindau protein in epithelial ovarian neoplasms and allelic loss of von Hippel-Lindau gene: nuclear expression of hypoxia-inducible factor 1alpha is an independent prognostic factor in ovarian carcinoma. *Hum Pathol* 38: 1310–1320

Palazon A, Martinez-Forero I, Teijeira A, Morales-Kastresana A, Alfaro C, Sanmamed MF, Perez-Gracia JL, Penuelas I, Hervas-Stubbs S, Rouzaut A *et al* (2012) The HIF-1alpha hypoxia response in tumor-infiltrating T lymphocytes induces functional CD137 (4–1BB) for immunotherapy. *Cancer Discov* 2: 608–623

Palazon A, Tyrakis PA, Macias D, Velica P, Rundqvist H, Fitzpatrick S, Vojnovic N, Phan AT, Loman N, Hedenfalk I *et al* (2017) An HIF-1alpha/VEGF-A axis in cytotoxic T cells regulates tumor progression. *Cancer Cell* 32: 669–683

Pangou E, Befani C, Mylonis I, Samiotaki M, Panayotou G, Simos G, Liakos P (2016) HIF-2alpha phosphorylation by CK1delta promotes erythropoietin secretion in liver cancer cells under hypoxia. *J Cell Sci* 129: 4213–4226

Ramakrishnan SK, Zhang H, Takahashi S, Centofanti B, Periyasamy S, Weisz K, Chen Z, Uhler MD, Rui L, Gonzalez FJ *et al* (2016) HIF2alpha is an essential molecular brake for postprandial hepatic glucagon response independent of insulin signaling. *Cell Metab* 23: 505–516

Rankin EB, Giaccia AJ (2016) Hypoxic control of metastasis. *Science* 352: 175–180

Seidel S, Garvalov BK, Wirta V, von Stechow L, Schanzer A, Meletis K, Wolter M, Sommerlad D, Henze AT, Nister M *et al* (2010) A hypoxic niche regulates glioblastoma stem cells through hypoxia inducible factor 2 alpha. *Brain* 133: 983–995

Semenza GL (2012) Hypoxia-inducible factors in physiology and medicine. *Cell* 148: 399–408

Semenza GL (2016) Dynamic regulation of stem cell specification and maintenance by hypoxia-inducible factors. *Mol Aspects Med* 47–48: 15–23

Shukla SK, Purohit V, Mehla K, Gunda V, Chaika NV, Vernucci E, King RJ, Abrego J, Goode GD, Dasgupta A *et al* (2017) MUC1 and HIF-1alpha signaling crosstalk induces anabolic glucose metabolism to impart gemcitabine resistance to pancreatic cancer. *Cancer Cell* 32: 71–87

Stalmans S, Bracke N, Wynendaele E, Gevaert B, Peremans K, Burvenich C, Polis I, De Spiegeleer B (2015) Cell-penetrating peptides selectively cross the blood-brain barrier *in vivo*. *PLoS One* 10: e0139652

Stegen S, Laperre K, Eelen G, Rinaldi G, Fraisl P, Torrekens S, Van Looveren R, Loopmans S, Bultynck G, Vinckier S *et al* (2019) HIF-1alpha metabolically controls collagen synthesis and modification in chondrocytes. *Nature* 565: 511–515

Sun P, Lu YX, Cheng D, Zhang K, Zheng J, Liu Y, Wang X, Yuan YF, Tang YD (2018) Monocyte chemoattractant protein-induced protein 1 targets hypoxia-inducible factor 1alpha to protect against hepatic ischemia/reperfusion injury. *Hepatology* 68: 2359–2375

Tanimoto K, Makino Y, Pereira T, Poellinger L (2000) Mechanism of regulation of the hypoxia-inducible factor-1 alpha by the von Hippel-Lindau tumor suppressor protein. *EMBO J* 19: 4298–4309

Thorne C, Eccles RL, Coulson JM, Urbe S, Clague MJ (2011) Isoform-specific localization of the deubiquitinase USP33 to the Golgi apparatus. *Traffic* 12: 1563–1574

Tian H, McKnight SL, Russell DW (1997) Endothelial PAS domain protein 1 (EPAS1), a transcription factor selectively expressed in endothelial cells. *Genes Dev* 11: 72–82

Troilo A, Alexander I, Muehl S, Jaramillo D, Knobeloch KP, Krek W (2014) HIF1alpha deubiquitination by USP8 is essential for ciliogenesis in normoxia. *EMBO Rep* 15: 77–85

van den Beucken T, Koch E, Chu K, Rupaimoole R, Prickaerts P, Adriaens M, Voncken JW, Harris AL, Buffa FM, Haider S *et al* (2014) Hypoxia promotes stem cell phenotypes and poor prognosis through epigenetic regulation of DICER. *Nat Commun* 5: 5203

Vordermark D, Shibata T, Brown JM (2001) Green fluorescent protein is a suitable reporter of tumor hypoxia despite an oxygen requirement for chromophore formation. *Neoplasia* 3: 527–534

West XZ, Malinin NL, Merkulova AA, Tischenko M, Kerr BA, Borden EC, Podrez EA, Salomon RG, Byzova TV (2010) Oxidative stress induces angiogenesis by activating TLR2 with novel endogenous ligands. *Nature* 467: 972–976

Wu HT, Kuo YC, Hung JJ, Huang CH, Chen WY, Chou TY, Chen Y, Chen YJ, Chen YJ, Cheng WC *et al* (2016) K63-polyubiquitinated HAUSP deubiquitinates HIF-1alpha and dictates H3K56 acetylation promoting hypoxia-induced tumour progression. *Nat Commun* 7: 13644

Yan Q, Bartz S, Mao M, Li L, Kaelin Jr WG (2007) The hypoxia-inducible factor 2alpha N-terminal and C-terminal transactivation domains cooperate to promote renal tumorigenesis *in vivo*. *Mol Cell Biol* 27: 2092–2102

Yuasa-Kawada J, Kinoshita-Kawada M, Wu G, Rao Y, Wu JY (2009) Midline crossing and Slit responsiveness of commissural axons require USP33. *Nat Neurosci* 12: 1087–1089

Zhang A, Tao W, Zhai K, Fang X, Huang Z, Yu JS, Solan AE, Rich JN, Zhou W, Bao S (2020) Protein sumoylation with SUMO1 promoted by Pin1 in glioma stem cells augments glioblastoma malignancy. *Neuro Oncol* 22: 1809–1821

Zhang C, Peng Z, Zhu M, Wang P, Du X, Li X, Liu Y, Jin Y, McNutt MA, Yin Y (2016) USP9X destabilizes pVHL and promotes cell proliferation. *Oncotarget* 7: 60519–60534

Zhou W, Chen C, Shi YU, Wu Q, Gimple RC, Fang X, Huang Z, Zhai K, Ke SQ, Ping Y-F *et al* (2017) Targeting glioma stem cell-derived pericytes disrupts the blood-tumor barrier and improves chemotherapeutic efficacy. *Cell Stem Cell* 21: 591–603

Zhuang Z, Yang C, Ryska A, Ji Y, Hou Y, Graybill SD, Bullova P, Lubensky IA, Kloppel G, Pacak K (2016) HIF2A gain-of-function mutations detected in duodenal gangliocytic paraganglioma. *Endocr Relat Cancer* 23: L13–L16

Zhuo H, Zhao Y, Cheng X, Xu M, Wang L, Lin L, Lyu Z, Hong X, Cai J (2019) Tumor endothelial cell-derived cadherin-2 promotes angiogenesis and has prognostic significance for lung adenocarcinoma. *Mol Cancer* 18: 34